

Chapter 12

Chaos Synchronization in Semiconductor Lasers

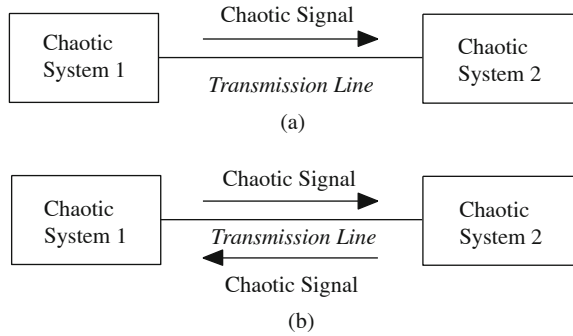
Another important application of chaotic semiconductor lasers is chaotic secure communications. The key to chaotic communications is chaos synchronization between two nonlinear systems. If two nonlinear chaotic systems operate independently, the two systems never show the same output because of the sensitivity of chaos for the initial conditions. However, when a small portion of a chaotic output from one nonlinear system is sent to the other, the two systems synchronize with each other and show the same output under certain conditions of the system parameters. This scheme is called chaos synchronization. It is very surprising that two chaotic systems share the same waveform, since chaos is sensitive to the initial conditions and its future is unpredictable. In this chapter, we overview chaos synchronization in chaotic semiconductor laser systems for the introduction of the secure chaos communications discussed in Chap. 13.

12.1 Concept of Chaos Synchronization

12.1.1 Chaos Synchronization

We cannot expect the same chaotic oscillation for two nonlinear systems even when they are the same configuration having the same parameter values, because chaos has strict sensitivity to the initial conditions of the parameters. For example, two chaotic systems with the same parameters may at first output similar signals when the difference between the initial conditions is small enough in the ordinary sense. Then, the two signals show a small difference with lapse of time and, then, the difference rapidly increases for further time development. Finally, the two systems behave in a completely different manner in as far as the difference between the initial conditions is not zero. However, there is a possibility of showing the same output in two nonlinear systems if the two systems possess a common subsystem with the same parameter values, otherwise if a small amount of the signal from one of the

Fig. 12.1 General idea of chaos synchronization of a one-to-one transmitter–receiver system



two systems is transmitted to the other. Under this condition, the systems output completely the same chaotic signal. The scheme is called “chaos synchronization.”

The idea of chaos synchronization between two nonlinear systems was proposed by Pecora and Carroll in 1990 (Pecora and Carroll 1990, 1991). They used a Lorenz system with three variables for the demonstration. In their system, an output from one of the variables as a subsystem in a transmitter was sent to a receiver. Then, they showed chaotic synchronization between the transmitter and receiver systems. After their proposal, synchronization phenomena in various chaotic systems including lasers have been reported. The idea and principle of chaos synchronization are described in Appendix A.4. Chaos synchronization between two nonlinear systems is not self-evident and this is a real surprise, since we cannot expect the same output even for the same two chaotic systems as far as the two systems are isolated from each other. The origin of chaos synchronization has not been fully understood yet and the theoretical background has not been established. However, chaos synchronization has been observed by numerical simulations and experiments in various nonlinear systems. In laser systems, synchronization of chaos was experimentally demonstrated in CO₂ lasers (Sugawara et al. 1994) and solid-state lasers (Roy and Thornburg 1994). After that, many theoretical and experimental researches for chaos synchronization in various laser systems including semiconductor lasers were published.

Here, we show the general idea of chaos synchronization. Figure 12.1 is a one-to-one system of chaos synchronization. The receiver of chaotic system 2 consists of the same configuration as chaotic transmitter system 1 and also has the same device characteristics as those of system 1. A small portion of the transmitter output is sent to the receiver. In Fig. 12.1a, the transmitter signal is unidirectionally coupled to the receiver and the chaotic output from the receiver synchronizes with the transmitter under an appropriate condition. In laser systems, an optical isolator is usually used to realize unidirectional coupling and the laser output from the transmitter is optically injected to the receiver laser. As a matter of fact, transmitter and receiver lasers may not be the same types as chaotic light sources, or even the transmitter may not be the same kind of laser as the receiver laser. As far as the transmitter can simulate and transmit a possible chaotic waveform of the receiver laser with the same optical frequency, successful chaos synchronization can be achieved. Indeed, a virtual

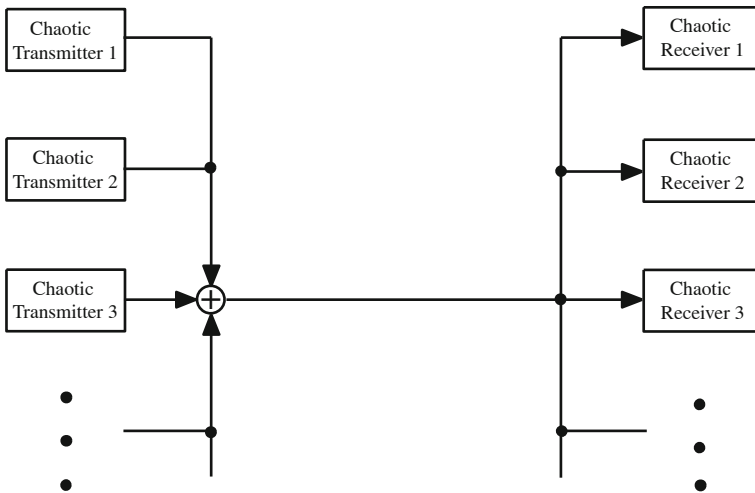


Fig. 12.2 Multiple transmitter–receiver systems of chaos synchronization

chaotic waveform numerically simulated by a computer is also used as a transmitter signal to a real receiver laser for chaos synchronization. Chaos synchronization is realized for a negative value of the maximum conditional Lyapunov exponent for the difference between the transmitter and receiver signals. Figure 12.1b is a chaos synchronization system of the mutual coupling of signals. Unidirectional systems are mainly used for secure chaotic data communications, however, we can perform simultaneous data transmissions using mutual coupling systems and the properties of those systems have been studied as a chaos synchronization scheme.

Chaos synchronization is attained not only in one-to-one transmitter–receiver systems but also in the multiple transmitter–receiver systems shown in Fig. 12.2. In this system, all the transmitters and receivers may be the same system, but each transmitter laser exhibits different chaotic output from the others. In this case, the parameter values for each pair of the transmitter and receiver systems must be the same and they become the key for chaos synchronization. Otherwise, a transmitter is a different system from each other and one of the receivers may play a counterpart to the transmitter. Chaotic signals from the transmitters are sent through a single transmission line and broadcasted to each receiver. In the receiver systems, each chaotic signal from the transmitters only synchronizes with the corresponding receiver having the same system and device characteristics. Indeed, chaos synchronization has been demonstrated in a few of multiple transmitter–receiver systems (Liu and Davis 2000). Other examples are one-to-many and many-to-one optical chaos synchronization and communication systems (Zhang et al. 2008). They numerically demonstrated chaos synchronization in such systems and successfully recovered original messages both for one-to-many and many-to-one systems.

In the proposal of chaos synchronization by Pecora and Carroll, the system is divided into two subsystems. In their model, the transmitter has two subsystems,

while the receiver has only one of the two subsystems (for details, the reader is referred to Appendix A.4). The chaotic signal from one of the subsystems is transmitted to the receiver. Then, the receiver conforms the complete chaotic system by the signal transmission and the receiver synchronizes with the transmitter under an appropriate condition of the parameters. The idea of chaos synchronization was immediately applied in real electronic circuit systems after the proposal by Pecora and Carroll (Cuomo et al. 1993). However, the method is not straightforwardly applicable to laser systems, since we cannot divide the dynamics of laser variables into subsystems.

Chaos synchronization strategies developed for most nonlinear systems, such as nonlinear circuits, cannot be directly implemented on semiconductor lasers because of a number of significant differences between semiconductor lasers and other nonlinear dynamical systems. The differences are as follows:

1. A semiconductor laser is an integrated entity that cannot be easily decomposed into subsystems.
2. For a given laser, it is not possible to arbitrarily adjust its intrinsic dynamical parameters and they can be only varied through their linear dependence on the laser power by varying the bias point of the laser.
3. One of its dynamical variables, the carrier density, is not directly accessible externally and, therefore, cannot be used to couple the transmitter and receiver lasers for synchronization.
4. When the output laser field of the transmitter laser is transmitted and coupled to the receiver laser, both its magnitude and phase are transmitted and coupled. It is not possible to only transmit and couple the magnitude but not the phase, or only the phase but not the magnitude.

By using a driving signal to link two chaotic systems, synchronization can be achieved if the difference between the outputs of the two systems possesses a stable fixed point with zero value. As an alternative technique in laser systems, the difference between certain variables in transmitter and receiver lasers can be used as control parameters for synchronization (Annovazzi-Lodi et al. 1996). In semiconductor lasers, master–slave configurations are frequently used as chaos synchronization systems suitable for chaotic secure communications. The schemes of optical feedback, optical injection, and optoelectronic feedback are used as typical chaotic generators in semiconductor lasers. Chaos synchronization in particular systems is discussed in the subsequent sections in this chapter. They are mostly numerical demonstrations of chaos synchronization, however, several experimental results have been reported.

12.1.2 Generalized and Complete Chaos Synchronization

There are two different origins of chaos synchronization in nonlinear delay differential systems, such as in semiconductor laser systems of optical feedback and optoelectronic feedback. One is synchronization of chaotic signals based on

optical injection phenomena. The other is complete chaos synchronization in which the two systems can be written by a set of the identical rate equations in a mathematical sense. We will discuss the two synchronization schemes in this section. In the ordinary sense, chaos synchronization occurs immediately after a receiver receives a chaotic signal from a transmitter when the transmitter and receiver are divided into several subsystems (see Appendix A.4). In this case, the time lag of the signal in the receiver system is defined by time τ_c , which is the transmission time of signal from the transmitter to the receiver. Namely, using the chaotic signals $\mathbf{y}(t)$ and $\mathbf{y}'(t)$ from the transmitter and receiver systems, respectively, the relation

$$\mathbf{y}'(t) = K_p \mathbf{y}(t - \tau_c) \quad (12.1)$$

is obtained (Ohtsubo 2002a). In (12.1), K_p is the proportional coefficient, and \mathbf{y} and \mathbf{y}' are essentially vector variables. In laser systems, this type of chaos synchronization is achieved by optical injection locking and amplification of signals from the transmitter to the receiver. This is the well-known phenomenon of injection locking in laser systems. The receiver output is usually an amplified signal of the transmitted signal (the gain is not necessary larger than unity). Therefore, an excellent synchronized waveform is obtained in the receiver system when the amplification is faithfully achieved. However, distortions are usually introduced to the injection-locked waveforms and the correlation between the transmitter and receiver outputs is less than unity. This scheme is called generalized synchronization.

On the other hand, there exists a different scheme of chaos synchronization from the generalized one in delay differential systems. We assume a system like a delay differential system such as optical feedback or optoelectronic feedback in a semiconductor laser. The differential equation in the transmitter output $\mathbf{y}(t)$ is described by

$$\frac{d\mathbf{y}(t)}{dt} = f(\mathbf{y}(t), \boldsymbol{\mu}_p) + \kappa_{p0} \mathbf{y}(t - \tau) \quad (12.2)$$

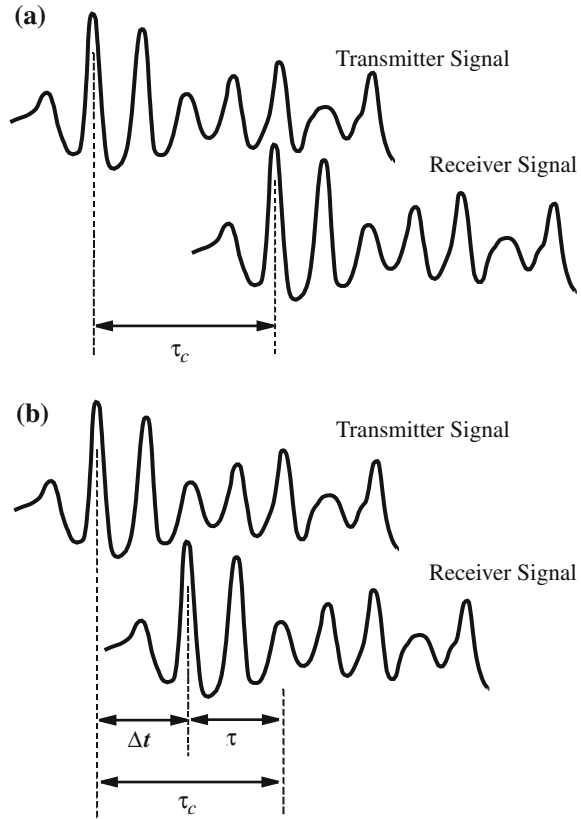
where $\boldsymbol{\mu}_p$ is the vector of chaos parameters, κ_{p0} is the feedback coefficient in the system, τ is the delay time, and f is the nonlinear function describing the delay differential system. Assuming that a small portion of the transmitter signal is sent to the receiver, the receiver equation is written by

$$\frac{d\mathbf{y}'(t)}{dt} = f(\mathbf{y}'(t), \boldsymbol{\mu}_p) + \kappa_{p1} \mathbf{y}'(t - \tau) + \kappa_{p2} \mathbf{y}(t - \tau_c) \quad (12.3)$$

where κ_{p1} is the feedback coefficient in the receiver system, κ_{p2} is the coupling coefficient between the transmitter and the receiver, τ_c is again the transmission time of the signal from the transmitter to the receiver. From a comparison between (12.2) and (12.3), we obtain the condition for the equivalent forms of the two differential equations as

$$\mathbf{y}'(t) = \mathbf{y}(t - \Delta\tau) \quad (12.4)$$

Fig. 12.3 Time lag between transmitter and receiver waveforms in chaos synchronization. Time lags **a** in generalized chaos synchronization and **b** in complete chaos synchronization. τ_c is the transmission time of the signal from the transmitter to the receiver and τ is the optical feedback time in the transmitter and receiver systems



$$\Delta t = \tau_c - \tau \tag{12.5}$$

$$\kappa_{p0} = \kappa_{p1} + \kappa_{p2} \tag{12.6}$$

Under the above conditions, the receiver system is mathematically described by the equivalent equation such as that of the transmitter system and the receiver generates completely the same output as the transmitter (not an amplified signal but a complete copy of the transmitter signal), since the two systems possess the same seeding signal through the coupling. Therefore, the synchronization scheme is called complete chaos synchronization and it is distinguished from generalized synchronization of chaotic oscillations. The above examples are of chaos synchronization for unidirectionally coupled nonlinear systems. However, we can consider mutually coupled systems for chaos synchronization. In that case, there are also two types of chaos synchronization, i.e., generalized and complete schemes. We will discuss chaos synchronization in mutually coupled laser systems later in this chapter.

The difference between the complete and generalized synchronization is clear from (12.1) and (12.4) and the scheme of chaos synchronization in a particular system is easily distinguished by investigating the time lag between the transmitter and receiver outputs. Figure 12.3 shows the relations of time lags in the two schemes. The receiver outputs a synchronized waveform immediately after it receives the transmitter signal in generalized chaos synchronization in Fig. 12.3a. Therefore, the time lag between the two outputs is τ_c . On the other hand, a synchronous chaotic signal in the receiver is generated in advance to receiving the transmitter signal for complete chaos synchronization as shown in Fig. 12.3b. The time lag $\Delta\tau$ in the complete chaos synchronization is less than the signal transmission between the transmitter and receiver systems. Complete chaos synchronization is sometimes called anticipating chaos synchronization due to its origin (Masoller 2001). However, it has been proved that anticipating chaos synchronization is not a unique phenomenon in delay differential systems, but also it is universally observed in differential systems. Indeed, Voss (2000) demonstrated anticipating chaos synchronization in a Rössler system that is described by a set of simple differential equations. Further, it is proved that anticipating chaos synchronization is not equivalent to complete chaos synchronization. Kusumoto and Ohtsubo (2003) observed anticipating chaos synchronization based on the injection-locking phenomenon in semiconductor lasers with optical feedback. The investigation of chaos synchronization for the mathematical and physical backgrounds is still undergoing and many subjects are left for future study.

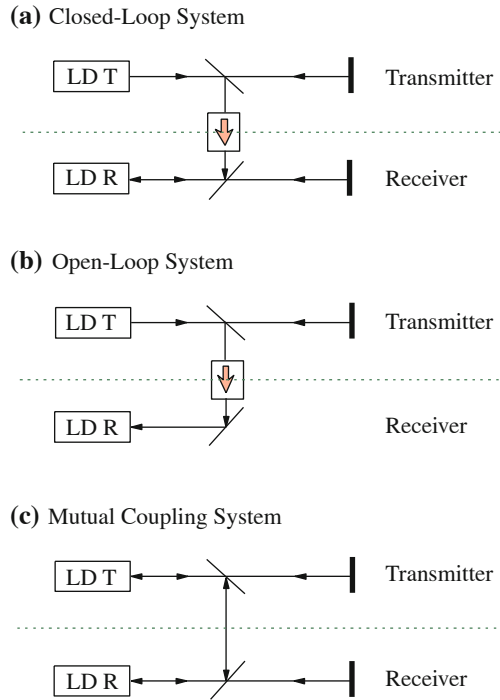
12.2 Theory of Chaos Synchronization in Semiconductor Lasers with Optical Feedback

12.2.1 Model of Synchronization Systems

There are two schemes of chaos synchronization in delay differential systems. A semiconductor laser subjected to optical feedback is a delay differential system and different dynamics like the Lorenz system are observed (see Appendix A.4). The systems of semiconductor lasers with optical feedback have been frequently used for chaotic generators in chaos synchronization and numerous reports have been published (Ohtsubo 2002b; Uchida et al. 2005 and the references therein). In the following, detailed explanations of synchronization in chaotic semiconductor lasers subjected to optical feedback are given. Examples for some other systems will be presented later.

In laser systems, a small portion of the output from one of variables (usually the laser output power or the complex field) is sent to the receiver laser instead of sharing common variables. Chaos synchronization is very sensitive to parameter mismatches between the transmitter and receiver systems. For example, even for semiconductor lasers coming from the same wafer, we cannot expect exactly the same oscillation frequencies for the transmitter and receiver lasers under the same

Fig. 12.4 Schematic diagram of chaos synchronization systems in semiconductor lasers with optical feedback. **a** Symmetric unidirectional coupling system, **b** asymmetric unidirectional coupling system, and **c** mutual coupling system. LD T: transmitter laser, LD R: receiver laser



bias injection current. That is in itself a reason why chaos synchronization is difficult to achieve in laser systems. However, laser frequency is easily tuned by changing the bias injection current and a slave laser frequency can be locked to a master laser by optical injection within a certain range of the frequency detuning. Therefore, we can achieve robust chaos synchronization using the frequency-pulling effect by carefully choosing the parameter conditions.

Chaos synchronization is achieved not only in a master–slave configuration of transmitter and receiver systems but also in a mutual coupling system (Fujino and Ohtsubo 2001; Heil et al. 2001). We can see complicated dynamics in mutual coupling systems compared with those in unidirectionally coupled systems. A few studies have been reported for chaos synchronization in mutual coupling systems and the study is still undergoing. We can still apply mutual coupling systems to chaotic secure communications, but some modifications of data transfers between transmitter and receiver lasers from that of unidirectional systems are necessary. The topic is treated in Chap. 13. As other applications of mutually coupled systems, they are used for phase locking and control of laser arrays (Winful and Rahman 1990; Sauer and Kaiser 1998; Garcia-Ojalvo et al. 1999). Chaos synchronization has been extensively studied in class B lasers and many experimental results have been reported. The semiconductor laser with optical feedback is the excellent model of chaos synchronization both for the theoretical and experimental studies.

We here discuss systems for chaos synchronization in semiconductor lasers with optical feedback (Ohtsubo 2002a). Figure 12.4 schematically shows the chaos synchronization systems. Figure 12.4a shows a unidirectional coupling system in which the receiver laser is isolated from the transmitter laser by an optical isolator. Both the transmitter and receiver systems have optical feedback loops and this configuration is called a closed-loop system. In Fig. 12.4b, the system is also a unidirectional coupling, but the receiver system does not have a feedback loop. This asymmetric system is called an open-loop system. The robustness and accuracy of chaos synchronization in the open-loop system are quite different from those in the closed-loop system. In chaos synchronization, the transmitter must output a chaotic signal. However, the receiver systems may or may not be chaotic without receiving the transmitter signal. Chaos synchronization is achieved by an injection of a chaotic signal. As a matter of fact, Fig. 12.4b shows a special case of Fig. 12.4a. Indeed, the system in Fig. 12.4a reduces to the system in Fig. 12.4b, when we put the reflectivity of the external reflector equal to zero. We mostly discuss chaos synchronization for the closed-loop configuration of Fig. 12.4a, but the open-loop system is implicitly included in the discussion. Figure 12.4c is a mutual coupling system. Here, the isolator in Fig. 12.4a is removed. Then, each laser behaves as a transmitter and a receiver. In this system, each laser outputs different chaotic signals or steady-state signals before coupling. After the coupling, the two lasers output the same chaotic signal. In mutual coupling systems, chaotic oscillations, and chaos synchronization are also possible without the use of external mirrors. Namely, chaotic oscillations both for transmitter and receiver lasers can be attained when the two lasers directly couple with each other and one of the lasers plays a kind of a role for external mirror to the counterpart laser. Also an open-loop system is another option for mutual coupling configuration. There are also two synchronization schemes (complete and generalized schemes) in the mutual coupling case.

12.2.2 Rate Equations in Unidirectional Coupling Systems

In this section, we investigate the theoretical treatment for chaos synchronization in the unidirectional coupling closed-loop system shown in Fig. 12.4a. The rate equations for the transmitter and receiver lasers are written by the same equations as those for the model discussed in Chap. 4 except for the light transmission term in the receiver rate equations (Ahlers et al. 1998). The rate equations for the transmitter laser are written by

$$\frac{dA_T(t)}{dt} = \frac{1}{2} G_{n,T} \{n_T(t) - n_{th,T}\} A_T(t) + \frac{\kappa_T}{\tau_{in,T}} A_T(t - \tau_T) \cos \theta_T(t) \quad (12.7)$$

$$\frac{d\phi_T(t)}{dt} = \frac{1}{2} \alpha_T G_{n,T} \{n_m(t) - n_{th,T}\} - \frac{\kappa_T}{\tau_{in,T}} \frac{A_T(t - \tau_T)}{A_T(t)} \sin \theta_{PT}(t) \quad (12.8)$$

$$\frac{dn_T(t)}{dt} = \frac{J_T}{ed} - \frac{n_T(t)}{\tau_{s,T}} - G_{n,T}\{n_T(t) - n_{0,T}\}A_T^2(t) \quad (12.9)$$

$$\theta_T(t) = \omega_{0,T}\tau + \phi_T(t) - \phi_T(t - \tau_T) \quad (12.10)$$

where subscript T represents the transmitter laser. The rate equations for the receiver laser read

$$\begin{aligned} \frac{dA_R(t)}{dt} = & \frac{1}{2}G_{n,R}\{n_R(t) - n_{th,R}\}A_R(t) \\ & + \frac{\kappa_R}{\tau_{in,R}}A_R(t - \tau_R)\cos\theta_R(t) + \frac{\kappa_{cp}}{\tau_{in,R}}A_T(t - \tau_c)\cos\xi_c(t) \end{aligned} \quad (12.11)$$

$$\begin{aligned} \frac{d\phi_R(t)}{dt} = & \frac{1}{2}\alpha_R G_{n,R}\{n_R(t) - n_{th,R}\} - \frac{\kappa_R}{\tau_{in,R}}\frac{A_R(t - \tau_R)}{A_R(t)}\sin\theta_R(t) \\ & - \frac{\kappa_{cp}}{\tau_{in,R}}\frac{A_T(t - \tau_c)}{A_R(t)}\sin\xi_c(t) \end{aligned} \quad (12.12)$$

$$\frac{dn_R(t)}{dt} = \frac{J_R}{ed} - \frac{n_R(t)}{\tau_{s,R}} - G_{n,R}\{n_R(t) - n_{0,R}\}E_R^2(t) \quad (12.13)$$

$$\theta_R(t) = \omega_{0,R}\tau + \phi_R(t) - \phi_R(t - \tau_R) \quad (12.14)$$

$$\xi_c(t) = \omega_{0,T}\tau_c + \phi_R(t) - \phi_T(t - \tau_c) + \Delta\omega t \quad (12.15)$$

where subscript R denotes the receiver lasers, κ_{cp} is the injection rate from the transmitter to the receiver laser, and $\Delta\omega$ is the angular frequency detuning. The last terms in (12.11) and (12.12) are the effect of the chaotic signal from the transmitter. When the external feedback is zero in the receiver system, i.e., $\kappa_R = 0$, the model reduces to the open-loop system in Fig. 12.4b.

12.2.3 Generalized Chaos Synchronization

One of the origins of chaos synchronization in a semiconductor laser with optical feedback is the injection-locking and amplification phenomenon in a system modeled by delay differential equations. The condition for complete chaos synchronization, which is discussed in the next subsection, is very strict and most cases of chaos synchronization observed in lasers are based on the injection-locking and amplification phenomenon. Therefore, experimental results of chaos synchronization in laser systems were mostly for generalized chaos synchronization. We here consider the condition for the generalized chaos synchronization in a system of a semiconductor laser with optical feedback. For generalized chaos synchronization, the average

optical power injected to the receiver laser is large, as much as several tens of percent in amplitude (several percent in intensity), while it is much less than several percents for the case of complete chaos synchronization. In generalized chaos synchronization, the relation between the field amplitudes for the transmitter and receiver lasers is given by

$$A_R(t) \propto A_T(t - \tau_c) \quad (12.16)$$

Namely, the synchronized chaotic output in the receiver is generated upon receiving the transmitter signal. Therefore, the time lag between the outputs of the transmitter and receiver lasers is equal to the transmission time τ_c .

12.2.4 Complete Chaos Synchronization

Next, we consider the conditions where the two systems of the transmitter and receiver lasers are written by the identical set of equations, namely, the conditions for complete chaos synchronization. The model of chaotic generators for the transmitter and the receiver is also a semiconductor laser with optical feedback. We assume that the device parameters in the two lasers are the same and the two lasers oscillate at the same frequency, i.e., zero frequency detuning $\Delta\omega = \omega_{0,m} - \omega_{0,s} = 0$. Further, the lasers are biased at the same injection current and the external feedback conditions are also the same for the transmitter and receiver lasers, except for different values of the feedback coefficients, κ_T and κ_R . Under these assumptions, the conditions for complete chaos synchronization read (Ohtsubo 2002b)

$$A_R(t) = A_T(t - \Delta t) \quad (12.17)$$

$$\phi_R(t) = \phi_T(t - \Delta t) - \omega_0 \Delta t \pmod{2\pi} \quad (12.18)$$

$$n_R(t) = n_T(t - \Delta t) \quad (12.19)$$

$$\kappa_R = \kappa_T + \eta_c \quad (12.20)$$

$$\Delta t = \tau_c - \tau \quad (12.21)$$

The delay differential Eqs. (12.11)–(12.13) in the receiver laser have completely identical forms to those in (12.7)–(12.9) of the transmitter laser. The scheme is called complete chaos synchronization. The receiver laser outputs the synchronous chaotic signal before receiving the transmitted signal by anticipating it in advance to the time $\tau = \tau_T = \tau_R$. The parameters in the two laser systems must be identical to satisfy the conditions for complete chaos synchronization, however, there are certain ranges of tolerances for the parameter mismatches when we allow a little deterioration of the correlation between the transmitter and receiver outputs. Usually, it is not easy to achieve complete chaos synchronization in real laser systems, especially in

delay optical feedback systems, and a few experimental studies for complete chaos synchronization have been reported (Liu et al. 2002).

12.2.5 Mutual Coupling Systems

We discuss chaos synchronization in mutually coupled semiconductor lasers modeled in Fig. 12.4c. For simplicity, we put the reflectivities of external mirrors in the transmitter and receiver systems equal to zero without loss of generality, i.e., we remove the external mirrors. In the mutual coupling system, each laser plays a role for the virtual external mirror to the counterpart laser. Therefore, even without the optical feedback loop, the lasers can show chaotic oscillations due to mutual optical injections, as discussed in Chap. 6. Mutual coupling lasers with optical feedback is a straightforward extension of the discussion here. We can also observe both complete and generalized chaos synchronization in mutually coupled semiconductor lasers (Hohl et al. 1997, 1999). The rate equations for one of the lasers are written by

$$\frac{dA_1(t)}{dt} = \frac{1}{2}G_{n,1}\{n_1(t) - n_{th,1}\}A_1(t) + \frac{\kappa_{inj,2}}{\tau_{in,1}}A_2(t - \tau_c) \cos \theta_1(t) \quad (12.22)$$

$$\frac{d\phi_1(t)}{dt} = \frac{1}{2}\alpha_1 G_{n,1}\{n_1(t) - n_{th,1}\} - \frac{\kappa_{inj,2}}{\tau_{in,1}} \frac{A_2(t - \tau_c)}{A_1(t)} \sin \theta_1(t) \quad (12.23)$$

$$\frac{dn_1(t)}{dt} = \frac{J_1}{ed} - \frac{n_1(t)}{\tau_s,1} - G_{n,1}\{n_1(t) - n_{0,1}\}A_1^2(t) \quad (12.24)$$

$$\theta_1(t) = \omega_{0,1}\tau + \phi_1(t) - \phi_2(t - \tau_c) + \Delta\omega t \quad (12.25)$$

The rate equations for the other laser are also given by symmetrical forms as

$$\frac{dA_2(t)}{dt} = \frac{1}{2}G_{n,2}\{n_2(t) - n_{th,2}\}A_2(t) + \frac{\kappa_{inj,1}}{\tau_{in,2}}A_1(t - \tau_c) \cos \theta_2(t) \quad (12.26)$$

$$\frac{d\phi_2(t)}{dt} = \frac{1}{2}\alpha_2 G_{n,2}\{n_2(t) - n_{th,2}\} - \frac{\kappa_{inj,1}}{\tau_{in,2}} \frac{A_1(t - \tau_c)}{A_2(t)} \sin \theta_2(t) \quad (12.27)$$

$$\frac{dn_2(t)}{dt} = \frac{J_2}{ed} - \frac{n_2(t)}{\tau_s,2} - G_{n,2}\{n_2(t) - n_{0,2}\}E_2^2(t) \quad (12.28)$$

$$\theta_2(t) = \omega_{0,2}\tau + \phi_2(t) - \phi_1(t - \tau_c) - \Delta\omega t \quad (12.29)$$

where subscripts 1 and 2 are for the respective lasers and $\Delta\omega = \omega_1 - \omega_2$ is the angular frequency detuning between the two lasers.

In the mutual coupling systems, there are also two solutions of chaos synchronization; one is based on injection-locking and amplification phenomena and the other is complete chaos synchronization. For the case of synchronization due to injection-locking, one of the two lasers plays the role of a master laser and the other is a slave. Then, the relation between the two amplitudes is written by

$$A_2(t) \propto A_1(t - \tau_c) \quad (12.30)$$

or

$$A_2(t - \tau_c) \propto A_1(t) \quad (12.31)$$

These are no exact solutions for (12.22)–(12.29) in a mathematical sense. However, these relations are confirmed by numerical simulations and experiments. Most cases of chaos synchronization observed in real experiments in mutually coupled semiconductor lasers are based on generalized chaos synchronization. In these cases, the optical transmission power is as large as several tens of percent of the average amplitude of the chaotic variation. The percentage is almost the same as that in a unidirectional coupling system of a generalized chaos synchronization scheme. Which laser becomes master or slave (leader or lagger laser) is determined by the differences of the operating conditions of the lasers and the parameter mismatches.

On the other hand, there is an identical solution for complete chaos synchronization in mutually coupled semiconductor lasers, since the transmitter and receiver systems have mathematically symmetrical forms as far as the device parameters and driving conditions are identical. The conditions follow

$$\Delta\omega = 0 \quad (12.32)$$

$$A_2(t) = A_1(t) \quad (12.33)$$

$$A_2(t) = A_1(t) \quad (12.34)$$

$$n_2(t) = n_1(t) \quad (12.35)$$

Namely, the two lasers simultaneously output the same chaotic signals even for a finite transmission time τ_c of light. The scheme is also considered as anticipating chaos synchronization. However, the complete chaos synchronization under the current configuration is only limited to the case without Langevin noises. In actual systems, there exist Langevin noises and the synchronization is fairly affected by the noises. An isochronal solution of complete chaos synchronization is easily reduced to an achronal state due to the presence of the noises in spite of highly symmetrical conditions of two mutually coupling lasers. The detail is again discussed in Sect. 12.7.1

12.3 Chaos Synchronization in Semiconductor Lasers with an Optical Feedback System

12.3.1 Chaos Synchronization—Numerical Examples

We here show some numerical simulations of chaos synchronization in the closed-loop systems shown in Fig. 12.4b. Figure 12.5 shows examples of generalized and complete chaos synchronization (Murakami and Ohtsubo 2002). Figure 12.5a shows a chaotic signal to be transmitted. Figure 12.5b shows the receiver output under the condition of generalized chaos synchronization and Fig. 12.5c shows the correlation plot between the waveforms of Fig. 12.5a, b. Figure 12.5d shows the receiver output under the condition of complete chaos synchronization and Fig. 12.5e is the correlation plot between the waveforms of Fig. 12.5a and d. The optical transmission power is 22% ($\kappa_{cp}/\tau_{in,R} = 74.9 \text{ ns}^{-1}$) in the generalized chaos synchronization. On the other hand, it is as small as 1.5×10^{-4} % ($\kappa_{cp}/\tau_{in,R} = 1.96 \text{ ns}^{-1}$) in the complete case. The time for the light transmission between the transmitter and receiver lasers is set to zero for simplicity in this figure. Therefore, the time lag between the two lasers is zero for generalized synchronization, while it is -1 ns for complete chaos synchronization. An excellent correlation between the transmitter and receiver outputs is obtained for the complete chaos synchronization. The difference of the time is exactly equal to the theoretically expected time lag $\Delta\tau$. Thus, we can distinguish the type of chaos synchronization by investigating the time lag between the transmission signal and the receiver output.

The attractors in the transmitter and receiver lasers show the same orbit under complete chaos synchronization, since the two systems follow completely the identical equations. Then, the receiver output traces the same orbit as that of the transmitter due to injection of a small seed from the transmitter. On the other hand, the receiver output is an amplified copy of the transmitter signal in generalized chaos synchronization. Therefore, the synchronized signal almost looks the same as the waveform of the transmitter, however, the chaotic attractor in the receiver laser has some deviations from that of the transmitter. Figure 12.6 shows chaotic attractors of the receiver laser in the phase space of the laser output power and the carrier density. Figure 12.6a is the chaotic attractor of the transmitter signal in Fig. 12.5a. Figure 12.6b is the chaotic attractor of the receiver output corresponding to Fig. 12.5b. The general view of the orbit is quite similar to Fig. 12.6a, but they are different. The extent of the orbit in Fig. 12.6b is slightly larger than that of Fig. 12.6a and the receiver signal is amplified. Also, the carrier density in Fig. 12.6b is lowered to less than the threshold by the strong optical injection from the transmitter laser and this results in the reduction of the gain. For the case of complete chaos synchronization in Fig. 12.5d, the chaotic orbit of the receiver laser is the same as in Fig. 12.6a. From these facts, generalized chaos synchronization is clearly a different phenomenon from complete chaos synchronization.

Optical injection is widely used for signal transmission from transmitter to receiver lasers in chaotic communications. When we consider optical injection, the stable

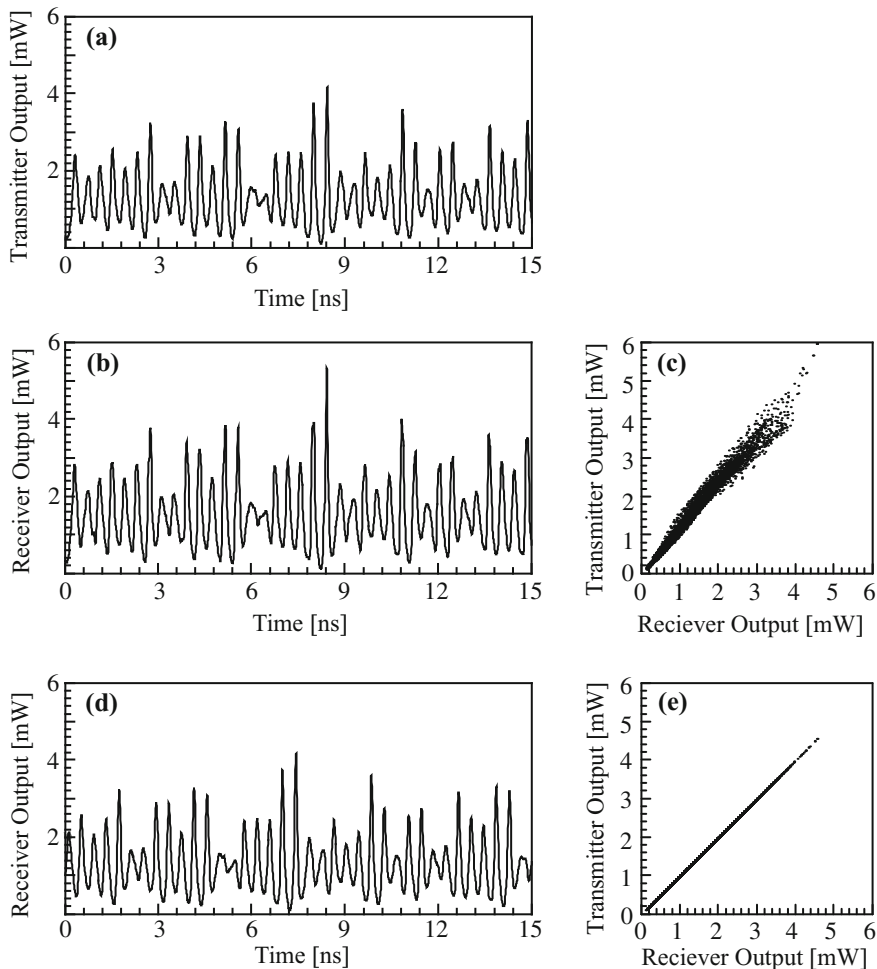


Fig. 12.5 Chaos synchronization in a closed-loop system. **a** Chaotic transmission signal, **b** receiver output of generalized chaos synchronization at $\kappa_{cp}/\tau_{in,R} = 74.9\text{ns}^{-1}$, **c** correlation plot for **a** and **b**, **d** receiver output of complete chaos synchronization at $\kappa_{cp}/\tau_{in,R} = 1.96\text{ns}^{-1}$, and **e** correlation plot for **a** and **d**. The conditions are $J = 1.3J_{th}$, $\tau = 1\text{ns}$, $\kappa_T/\tau_{in,T} = 1.96\text{ns}^{-1}$, and $\Delta\omega = 0$

and unstable map, which is discussed in Chap. 6, is very useful to know the injection properties. Here, we show the conditions and distributions of successful chaos synchronization using the map. Figure 12.7 presents the map of stable and unstable injection-locking areas. The boundaries of stable and unstable injection-locking, and unlocking for the solitary laser are shown as solid curves in the figure. The vertical axis is the optical injection (in intensity) from the transmitter to the receiver laser and the horizontal axis is the frequency detuning between the transmitter and receiver lasers. Excellent chaos synchronization is attained at the dark

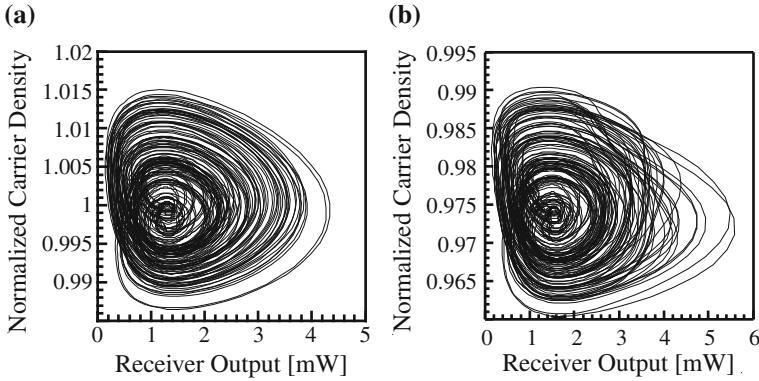
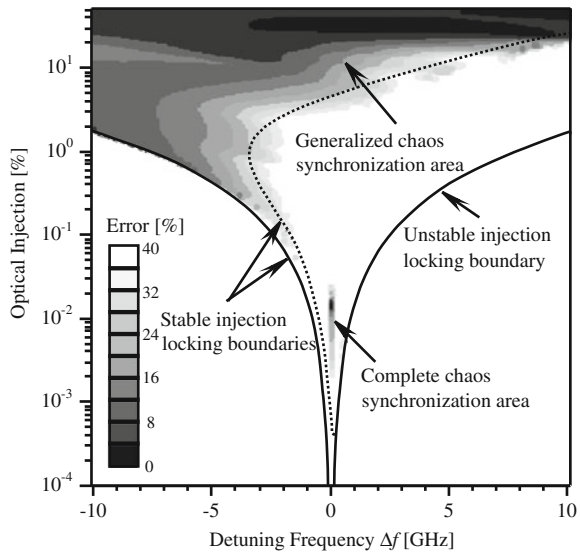


Fig. 12.6 Chaotic attractors in the phase space of laser output power and carrier density. **a** and **b** Chaotic attractors corresponding to Figs. 12.5b and d, respectively

Fig. 12.7 Map of stable and unstable injection locking in receiver laser and areas of generalized and complete chaos synchronization. An open-loop optical feedback system is assumed. The reflectivity of the external optical feedback mirror in the transmitter system is 10^{-2} % in intensity



areas in the map. The error of chaos synchronization in the figure is defined by the following equation:

$$\sigma_{\text{error}} = \frac{\langle |S_T - S_R| \rangle}{\langle S_R \rangle} \tag{12.36}$$

where S_T and S_R are the intensities of the transmitter and receiver lasers, and $\langle \cdot \rangle$ denotes the ensemble average. Generalized chaos synchronization occurs in a wide range of the frequency detuning and the optical injection in the stable injection-locking area, while complete chaos synchronization takes place at the unstable injection-locking area. From the comparison of this map with Fig. 6.6, complete

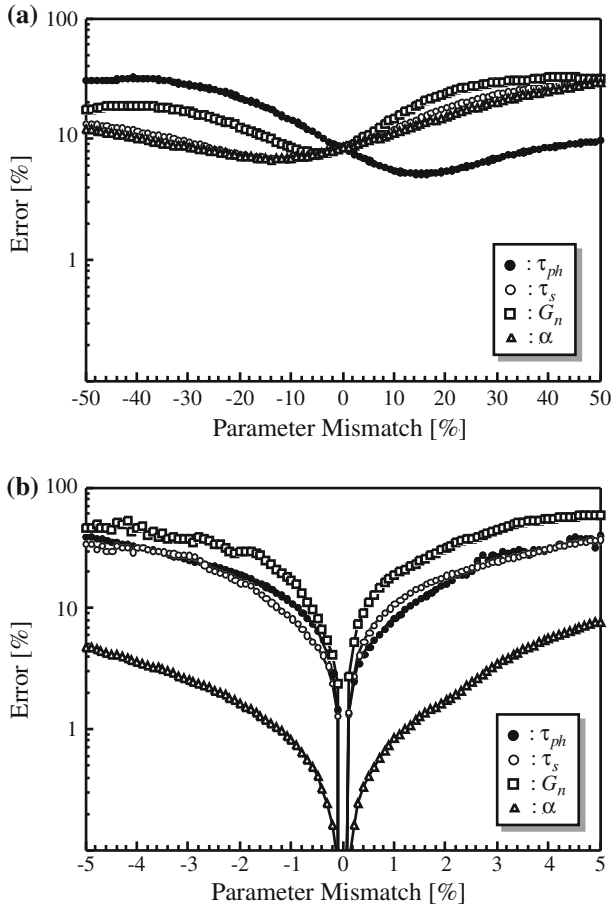


Fig. 12.8 Calculated synchronization error as a function of parameter mismatch. τ_{ph} : photon lifetime, τ_s : carrier lifetime, G_n : gain, and α : linewidth enhancement factor. **a** Generalized and **b** complete chaos synchronization. The parameter values are the same as those in Fig. 12.5

chaos synchronization is attained at chaotic states within the unstable injection-locking area in a simple optical injection-locked laser. The area of complete chaos synchronization is very narrow with zero detuning and small optical injection due to the requirement of strict parameter coincidence.

The effects of parameter mismatches between the transmitter and receiver systems are very important for applications of chaos synchronization to secure optical communications. Figure 12.8 shows the plots of synchronization errors for the mismatches of various laser device parameters. Figure 12.8a shows the errors of generalized chaos synchronization. The permissible errors for the parameter mismatches are large in generalized chaos synchronization and we can expect robust chaos synchronization. However, the synchronization errors are always larger than

1% of the average laser intensity variations, since the origin of the synchronization comes from optical injection-locking and amplification phenomena, and distortions of the synchronous waveform from the transmitter signal are always presented. From the investigation of the transmitter and receiver waveforms, they are still quite similar with each other when the errors for the parameter mismatches are less than a few percent. It is noted that the best synchronization is not always attained at zero parameter mismatches. Figure 12.8b is the effects of parameter mismatches in complete chaos synchronization. As expected, chaos synchronization is achieved with high accuracy at almost zero parameter mismatches and the synchronization errors rapidly increase with the increase of the parameter mismatches. Thus, strict conditions are required for successful chaos synchronization in the complete case.

12.3.2 Chaos Synchronization—Experimental Examples

Investigations on chaos semiconductor lasers with optical feedback have been reported in real experimental systems (Takiguchi et al. 1999a,b,c; Fujino and Ohtsubo 2000; Fischer et al. 2000a,b; Sivaprakasam et al. 2000). In this section, we show some examples of experimental results for chaos synchronization. Figure 12.9 shows the experimental results of chaos synchronization in a closed-loop system discussed in Fig. 12.4a. Figure 12.9a is the output waveforms of the transmitter and receiver lasers without signal transmission. As far as the two lasers are isolated, the output powers have no correlation as shown in Fig. 12.9b. When a fraction of the transmitter output is sent to the receiver, the synchronous waveform in Fig. 12.9c is obtained. The transmitted optical power from the transmitter to the receiver is rather strong, as much as 4.6% of the average power of the receiver laser. Therefore, the synchronization is a generalized case. In Fig. 12.9a, the two lasers show chaotic outputs. However, it is not always necessary for the receiver laser to be oscillated at a chaotic state and the receiver laser may be a steady-state oscillation even in the presence of optical feedback. The feedback level in the receiver laser is usually less than that in the transmitter laser and the receiver laser may show a synchronous chaotic oscillation after the optical injection from the transmitter. Chaos synchronization has been also demonstrated in an open-loop system. Of course, the receiver laser oscillates at a steady-state without coupling of the transmitter signal in that case. The robustness of chaos synchronization is much dependent on whether the system is an open- or closed-system. We will again discuss the differences in Chap. 13.

Only a few experimental studies have been reported for complete chaos synchronization, since the conditions of complete chaos synchronization are too severe to be achieved in real experiments (Sivaprakasam et al. 2001; Liu et al. 2002). At complete chaos synchronization, the time lag of the waveforms between the transmitter and receiver lasers is given by $\Delta\tau = \tau_c - \tau$. Liu et al. (2002) conducted complete chaos synchronization in an open-loop system of semiconductor lasers with optical feedback. They changed the external cavity length and examined the time lag between the transmitter and receiver signals. They observed the change of the time

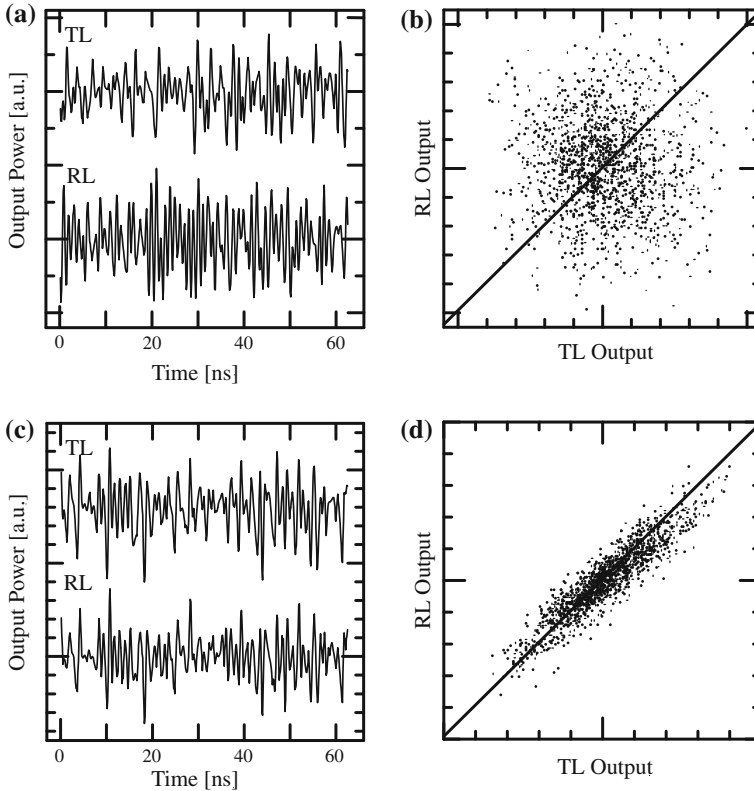


Fig. 12.9 Experimental chaos synchronization in a closed-loop system. **a** Waveforms of transmitter and receiver lasers without coupling. **b** Correlation plot for **a**. **c** Waveforms of transmitter and receiver lasers with coupling. The transmitted optical power is 4.6% of the average optical power of the receiver laser. **d** Correlation plot for **c**

lag proportional to the external cavity length (the proportional coefficient is negative) and showed that their schemes were for complete chaos synchronization. In their experiment, the parameters of the transmitter and receiver lasers were carefully chosen to have almost the same characteristics and the initial frequency detuning between the transmitter and receiver lasers was set to be less than several tens of MHz.

12.3.3 Anticipating Chaos Synchronization

Anticipating chaos synchronization was at first introduced as a synchronization phenomenon peculiar to nonlinear delay differential systems. Later, it was proved that anticipating chaos synchronization is also observed in low dimensional dissipative systems described by simple differential equations (Ahlers et al. 1998; Voss

2000; Ohtsubo 2002b). Voss demonstrated that anticipating chaos synchronization is realized in a Rössler system (continuous system) that is described by three differential equations. Therefore, anticipating chaos synchronization is not only a unique feature in delay differential systems, but also it is a universal phenomenon in chaotic nonlinear systems. In chaos synchronization systems of semiconductor lasers with optical feedback, anticipating chaos synchronization was also observed outside of the parameter regions for ordinary complete chaos synchronization in the stable and unstable injection-locking map. In that case, the chaos synchronization originated from optical injection-locking and amplification effects, but the time lag of the waveforms between the transmitter and receiver lasers was equal to that of anticipating synchronization.

Kusumoto and Ohtsubo (2003) conducted a detailed study of chaos synchronization in the stable injection-locking area in Fig. 12.7. Figure 12.10 shows their results. Figure 12.10a plots the anticipating chaos synchronization in the stable injection-locking area. The time lag corresponds to that of anticipating synchronization, but the synchronization originates from the ordinary injection-locking effect. Within the white ellipsoid in the figure, the value of the correlation coefficient between waveforms of the transmitter and receiver lasers exceeds 0.94. In this open-loop system, the optical feedback ratio in the transmitter system is as high as 0.3. Complete chaos synchronization is achieved around the optical injection rate of 0.3 at zero frequency detuning (marked A). Of course, the synchronization is an anticipating one under this condition. However, the area of anticipating chaos synchronization expands over a wide region in the stable injection-locking map. For example, the synchronization at point B is still an anticipating one as a time lag of the waveforms, but the synchronization originates from the injection-locking effect. Figure 12.10b plots the trajectories of the transmitter and receiver outputs corresponding to point B in Fig. 12.10a. The plot is in the phase space of the phase difference and the normalized carrier density. Black trace denotes the trajectory for the transmitter laser and gray trace is for the receiver laser. If the chaos synchronization is complete, the trajectory of the transmitter laser perfectly overlaps with that of the receiver in the map. However, the two trajectories are separated from each other in the phase space. This phase shift between the two trajectories is equal to the frequency detuning between the two lasers. Also the carrier density of the receiver laser is lowered by the optical injection. This fact proves that the phenomenon originates from optical injection-locking and amplification. According to the detailed study by Peters-Flynn et al. (2006), the laser output that is categorized as anticipating chaos synchronization in the stable injection-locking area in Fig. 12.10 sometimes shows a mixed state of waveforms corresponding to anticipating and injection amplification signals. The two states irregularly switch in time in their numerical simulations. The details of the phenomena and the origin of the switching are not fully understood yet. Anticipating chaos synchronization is not a unique phenomenon accompanying complete chaos synchronization, but it is a universal nature in nonlinear chaotic systems.

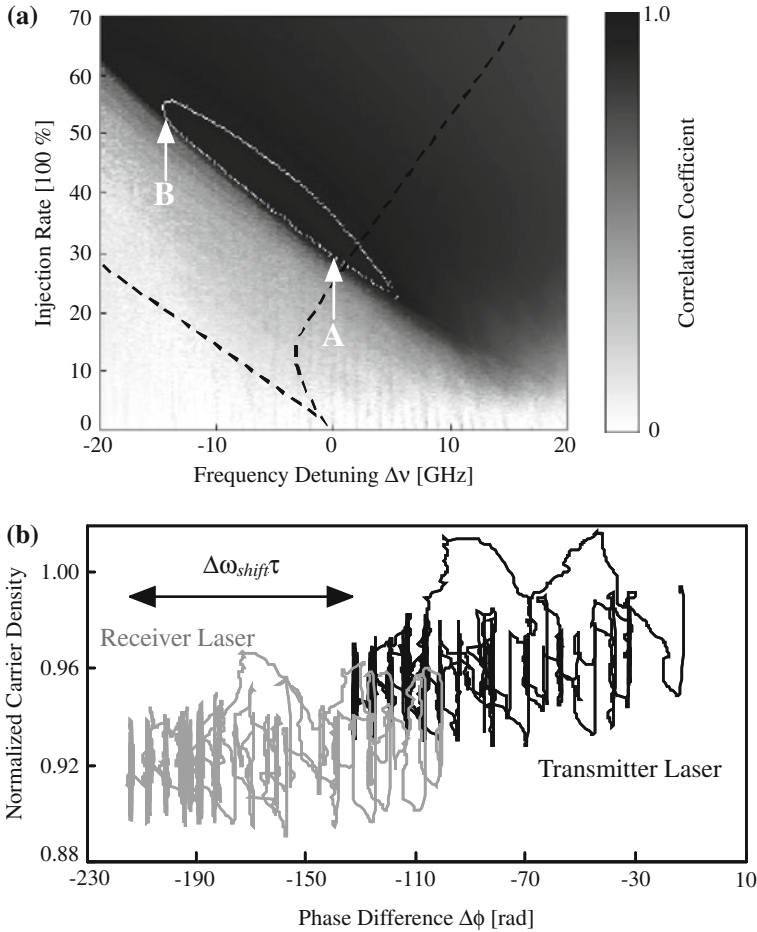


Fig. 12.10 **a** Anticipating chaos synchronization region in the phase space of frequency detuning $\Delta\nu$ and optical injection rate in the open-loop system. The feedback rate in the transmitter system is 0.3. **b** Chaotic trajectories for transmitter and receiver lasers at point B in **a**. The trajectories are plotted in the phase space of the phase difference $\Delta\phi = \phi_j(t) - \phi_j(t - \tau_t)$ and the normalized carrier density $n_j/n_{th,j}$ ($j = T$ or R). The *black* trace is for the transmitter laser and the *gray* trace for the receiver laser

12.3.4 Bandwidth Enhanced Chaos Synchronization

We discussed the enhancement of the cutoff frequency in a chaotic semiconductor laser by a strong optical injection in Sect. 6.3. Such semiconductor lasers are used as light sources of chaotic generators for chaos synchronization and communications (Takiguchi et al. 2003; Someya et al. 2009). The cutoff frequency can be varied by adjusting the fraction of the optical injection. For example, a modulation band-

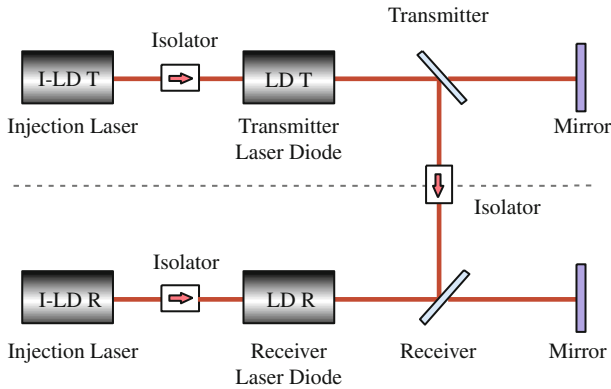
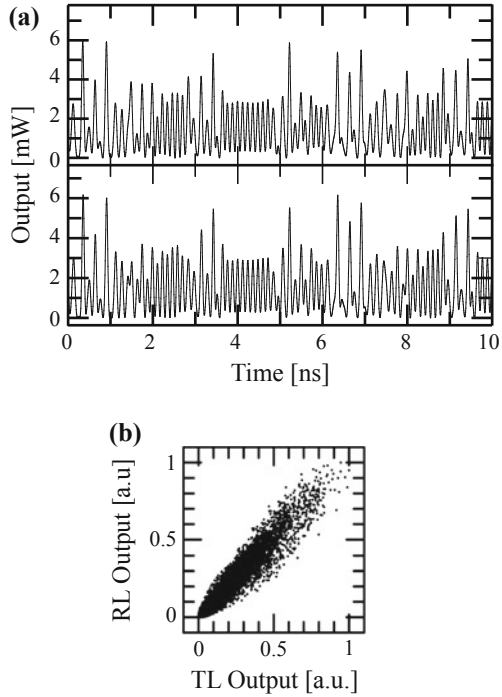


Fig. 12.11 Schematic diagram of bandwidth-enhanced chaos synchronization system. I-LD T and I-LD R are the injection lasers to the transmitter and receiver lasers. LD T and LD R are the transmitter and receiver lasers

width of ~ 20 GHz for the original relaxation oscillation frequency of 3–4 GHz was attained by strong optical injection. In chaotic communications, the maximum data transmission rate is determined by the cutoff frequency of chaotic carrier signals and the cutoff frequency is roughly equal to the maximum modulation bandwidth of the laser. Higher modulation bandwidth is also demanded in various applications such as direct modulations in semiconductor lasers. Figure 12.11 shows the schematic diagram of open-loop chaos synchronization systems with enhanced chaotic frequency (Takiguchi et al. 2003). Both the transmitter and receiver semiconductor lasers, LD T and LD R, are strongly injected from external semiconductor lasers, LD1 and LD2, with the same characteristics of the device parameters. Both the transmitter and receiver lasers oscillate at the stable injection-locked state in the absence of optical feedback. Figure 12.12 demonstrates an example of bandwidth-enhanced chaos synchronization. The conditions are the same as those in Fig. 6.20. Therefore, the main chaotic frequencies of the two lasers at solitary oscillations are 2.7 GHz and the main chaotic frequency is expanded to 8 GHz. The upper trace in Fig. 12.12a is a time series of the transmitter output and the lower one is that of the receiver. The frequency detuning between the transmitter and receiver lasers is set to be zero and the observed time lag is equal to $\Delta t = \tau_c - \tau = -6$ ns ($\tau_c = 0$ and $\tau = 6$ ns). Therefore, the synchronization scheme is for the complete case or so-called anticipating chaos synchronization. Figure 12.12b is the correlation plot. The correlation coefficient is calculated to be 0.954 and the two lasers show good synchronization. However, we obtain a better figure of the correlation coefficient for complete chaos synchronization in the absence of strong optical injection. The range for small synchronization error is very narrow for the parameter mismatches in the complete case. Even if the two lasers have the same device parameters and operate under the same conditions, chaos synchronization is realized under the limited parameter values and their ranges are usually very narrow.

Fig. 12.12 Bandwidth-enhanced chaos synchronization in semiconductor lasers with optical feedback. **a** Chaotic time series (upper trace; transmitter output and lower trace; receiver output) and **b** their correlation plot. The time lag of $\Delta t = -6\text{ns}$ between the two waveforms is compensated. The conditions for the lasers are the same as those in Fig. 6.20. The synchronization scheme is complete



12.3.5 Incoherent Synchronization Systems

The frequency detuning of the transmitter and receiver lasers plays a crucial role for the performance of chaos synchronization when the two lasers coherently couple. The difference of the frequencies must be at least within a few GHz. As discussed in Sect. 5.7, we can observe chaotic oscillations in systems of semiconductor lasers with incoherent optical feedback. Chaos synchronization is also realized in incoherent systems. We do not pay particular attention to the frequency detuning in this system. In an incoherent optical setup, the feedback light in the transmitter system is incoherently coupled with the internal laser field. We assume that the transmission light is also incoherently coupled to the receiver laser. In incoherent chaos synchronization, we do not need to consider the rate equation for the optical phase. Therefore, the model is described by the equations for the photon number and the carrier density. For the transmitter laser, we obtain (Register et al. 2001)

$$\frac{dS_T(t)}{dt} = G_{n,T}\{n_T(t) - n_{th,T}\}S_T(t) + R_{sp,T} \quad (12.37)$$

$$\begin{aligned} \frac{dn_T(t)}{dt} = & \frac{J_T}{ed} - \frac{n_T(t)}{\tau_{s,T}} - G_{n,T}\{n_T(t) - n_{0,T}\} \\ & \times \left\{ S_T(t) + \frac{\kappa_{T'}}{\tau_{in,s}} S_T(t - \tau_T) \right\} \end{aligned} \quad (12.38)$$

For the receiver

$$\frac{dS_R(t)}{dt} = G_{n,R}\{n_R(t) - n_{th,R}\}S_R(t) + R_{sp,R} \quad (12.39)$$

$$\begin{aligned} \frac{dn_R(t)}{dt} = & \frac{J_R}{ed} - \frac{n_R(t)}{\tau_{s,R}} - G_{n,R}\{n_R(t) - n_{0,R}\} \\ & \times \left\{ S_R(t) + \frac{\kappa_{R'}}{\tau_{in,R}} S_R(t - \tau_R) + \kappa_{cp} S_T(t - \tau_c) \right\} \end{aligned} \quad (12.40)$$

Also, the subscripts T and R are for the transmitter and receiver lasers. The feedback light is coupled to the carrier density as a delayed signal. The final term in (12.40) is the coupling of incoherent light from the transmitter. Since the coupling between the transmitter and receiver lasers is incoherent, the receiver laser is not injection-locked. However, complete chaos synchronization is also achieved under the appropriate conditions. Assuming all the device parameters of the two lasers to be the same, the conditions read

$$S_R(t) = S_T(t - \Delta t) \quad (12.41)$$

$$n_R(t) = n_T(t - \Delta t) \quad (12.42)$$

where $\Delta t = \tau_c - \tau$. Under these conditions, complete anticipating chaos synchronization is realized. Indeed, the condition for the frequencies of the lasers is not included in the coupling equations.

12.3.6 Polarization Rotated Chaos Synchronization

Chaotic oscillations of semiconductor lasers are observed not only by parallel-polarization optical feedback, but also by polarization-rotated optical feedback. The system of polarization-rotated optical was described in Sect. 4.6 and Sect. 5.8.1. The dynamics of polarization-rotated chaos synchronization were studied theoretically and experimentally (Sukow et al. 2004, 2005, 2006, Shibasaki et al. 2006; Takeuchi et al. 2010). A semiconductor laser with polarization-rotated optical feedback can be used as a light source for a system of chaotic synchronization and communications. Here, we discuss chaos synchronization in a system of semiconductor lasers with polarization-rotated optical feedback. As an example, take a chaotic generator shown in Fig. 4.7b. The system we consider is shown in Fig. 12.13, in which the laser light

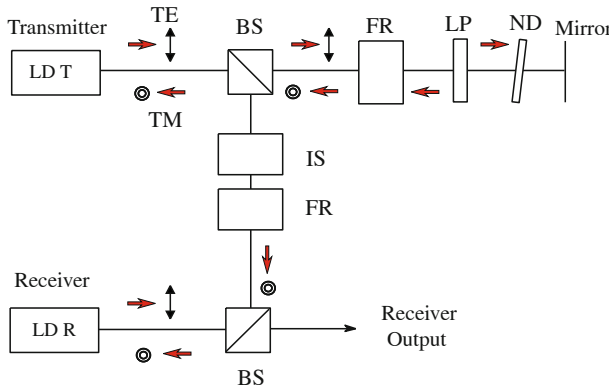


Fig. 12.13 System of polarization-rotated open-loop chaos synchronization system. LD T: transmitter laser, LD R: receiver laser, TE: TE polarization mode, TM: TM polarization mode, FR: Faraday rotator (45° rotation), IS: isolator, PL: polarizer, ND: neutral density filter

with TE mode emitted from a transmitter laser (LD T) passes through a Faraday rotator and is reflected by a mirror. The feedback light again passes through the Faraday rotator and fed back into the laser cavity as a TM mode light (cross-polarized component to the TE mode). A part of the TE mode light is divided by a beam splitter and is fed to the receiver laser through a set of an isolator and a Faraday rotator as the TM mode light. Then the crossed-polarization light is injected to the receiver laser. Thus, the polarization-rotated chaos synchronization is realized under appropriate conditions for the transmitter and receiver lasers.

In the open-loop chaos synchronization system in Fig. 12.13, the rate equations for the transmitter read (Shibasaki et al. 2006)

$$\frac{dE_{T,TE}(t)}{dt} = \frac{1}{2}(1 - i\alpha_T)G_{n,T,TE}\{n(t) - n_{th,T,TE}\}E_{T,TE}(t) \tag{12.43}$$

$$\begin{aligned} \frac{dE_{T,TM}(t)}{dt} &= \frac{1}{2}(1 - i\alpha_T)G_{n,T,TM}\{n(t) - n_{th,T,TM}\}E_{T,TM}(t) \\ &+ \frac{\kappa}{\tau_{in}}E_{T,TE}(t - \tau) \exp(-i\Delta\omega_{TE,TM}t + i\omega_0\tau + i\phi_{T,TM}(t) - i\phi_{T,TE}(t - \tau)) \end{aligned} \tag{12.44}$$

$$\begin{aligned} \frac{dn(t)}{dt} &= \frac{J_T}{ed} - \frac{n(t)}{\tau_{s,T}} - \{n(t) - n_{0,T}\} \\ &\times \left\{ G_{n,T,TE}|E_{T,TE}(t)|^2 + G_{n,T,TM}|E_{T,TM}(t)|^2 \right\} \end{aligned} \tag{12.45}$$

For the receiver systems, the rate equations are written by

$$\frac{dE_{R,TE}(t)}{dt} = \frac{1}{2}(1 - i\alpha_R)G_{n,R,TE}\{n(t) - n_{th,R,TE}\}E_{R,TE}(t) \quad (12.46)$$

$$\begin{aligned} \frac{dE_{R,TM}(t)}{dt} = & \frac{1}{2}(1 - i\alpha_R)G_{n,R,TM}\{n(t) - n_{th,R,TM}\}E_{R,TM}(t) \\ & + \frac{\kappa_{cp}}{\tau_{in,R}}E_{T,TE}(t - \tau_c) \exp(-i\Delta\omega t + i\omega_{0T}\tau + i\phi_{R,TM}(t) - i\phi_{T,TE}(t - \tau_c)) \end{aligned} \quad (12.47)$$

$$\begin{aligned} \frac{dn(t)}{dt} = & \frac{J_R}{ed} - \frac{n(t)}{\tau_{s,R}} - \{n(t) - n_{0,R}\} \\ & \times \{G_{n,R,TE}|E_{R,TE}(t)|^2 + G_{n,R,TM}|E_{R,TM}(t)|^2\} \end{aligned} \quad (12.48)$$

where subscripts TE and TM stand for two crossed polarization modes, subscript T and R correspond to for the transmitter and receiver lasers, $\Delta\omega_{TE,TM}$ represents the frequency detuning between TE and TM modes in the transmitter laser, $\Delta\omega$ is the frequency detuning between the transmitted light and the TM light in the receiver laser. The other parameters are the same meaning defined in Sect. 12.2.2. The dynamic properties of the transmitter and receiver lasers in polarization-rotated chaos synchronization are numerically studied by using these coupling equations. The frequency detuning between the TE and TM modes sometimes plays an important role, although it is usually small. Indeed, a frequency detuning of -870 MHz is experimentally observed and the dynamics and synchronization properties are fairly affected by the detuning (Takeuchi et al. 2010).

In transmitter and receiver systems in semiconductor lasers with polarization-rotated optical feedback, one can attain both regimes of chaos synchronization, i.e., complete and generalized cases. Figure 12.14 shows numerical examples of polarization-resolved waveforms both for complete and generalized chaos synchronization in polarization-rotated optical feedback regimes. It is noted that these are examples for zero frequency detuning between the TE and TM modes with fairly strong optical injection from TE to TM modes. When the injection ratio from the transmitter to the receiver lasers is equal to the optical feedback ratio in the transmitter laser, namely, $\kappa = \kappa_{cp}$, complete chaos synchronization can be achieved under appropriate parameter conditions, which is the same case for non-rotated optical feedback. For complete synchronization, the TE mode waveform of the transmitter laser completely synchronizes with the TE mode waveform of the receiver laser, and the TM mode of the response laser also synchronizes with the TM mode of the drive laser, as shown in Fig. 12.14a and c. Without loss of generality, the transmission time from the transmitter to the receiver lasers is equal to the delay time in the feedback loop in the transmitter, i.e., $\tau = \tau_c$. Therefore, the time lag between the synchronized signals is zero in complete chaos synchronization. In this configuration, the receiver

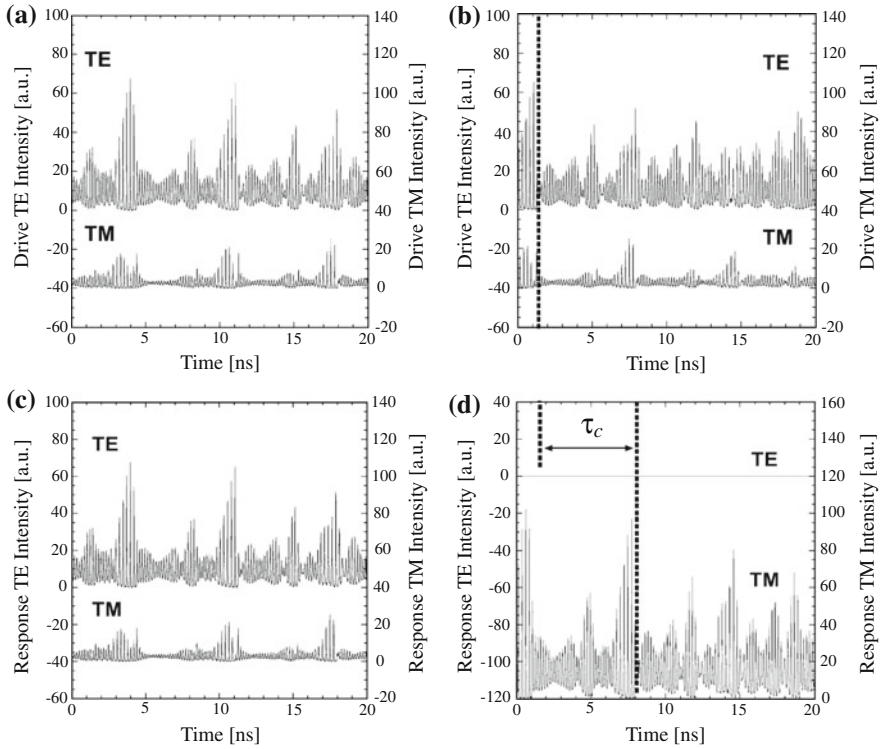


Fig. 12.14 Numerically calculated temporal waveforms of TE and TM mode intensities at synchronization. **a** and **c** Complete chaos synchronization for the transmitter and the receiver lasers, respectively, at $\kappa = \kappa_{cp}$. **b** and **d** Generalized chaos synchronization for the transmitter (drive) and the receiver (response) lasers, respectively, at $\kappa = 3\kappa_{cp}$. [after Shibasaki et al. (2006); © 2006 IEEE]

output is a complete copy of the transmitter signal. On the other hand, for a strong optical injection $\kappa = 3\kappa_{cp}$, the receiver laser is injection-locked to the transmitter laser. Then the receiver output of TM mode is an amplified version of the transmitted chaotic signal of the TE mode oscillation from the transmitter laser as shown in Fig. 12.14b and d. The time lag between the waveforms of the TE mode in the transmitter laser and the TM mode in the receiver laser is τ_c , which is the evidence of generalized chaos synchronization. In this example, the TE mode in the receiver laser is completely suppressed and only the TM polarization component is the oscillation mode.

As in the case for synchronization in semiconductor lasers with normal (non-polarization-rotated) optical feedback, the chaos in the two regimes (complete and generalized synchronization) are distinguishable by the delay of the chaotic waveform with respect to that of the injected signal. From the detailed study for polarization-rotated chaos synchronization, it is proved that chaos synchronization

can be performed even if there is a large mismatch in the optical frequencies of the lasers (Shibasaki et al. 2006). It is worth noting that synchronization can be maintained in the presence of the detuning by adjusting appropriately the injection strength between the transmitter and receiver lasers. This feature is very different from the case of semiconductor lasers with non-polarization-rotated optical feedback, where complete synchronization is only very weakly robust against detuning. Good synchronization can be maintained at the condition of positive detuning and small injection strength and at the condition of negative detuning and large injection strength. This asymmetric feature may result from the α parameter (linewidth enhancement factor) of semiconductor lasers, in the sense that chaos synchronization in semiconductor lasers with polarization-rotated optical feedback does not require strict matching of optical frequency. This feature of robustness with respect to optical frequency is particularly important for practical implementations of secure communication systems using chaos synchronization.

12.4 Chaos Synchronization in Injected Lasers

12.4.1 Theory of Chaos Synchronization in Injected Lasers

Semiconductor lasers exhibit chaotic oscillations by optical injection from a different laser as discussed in Chap. 6. We can use an optically injected laser as a light source for chaos synchronization as depicted in Fig. 6.1. However, an optical injection system is not a delay differential system, so that complete chaos synchronization is not generally realized in this system. We can also consider two types of synchronization systems; closed- and open-loop systems (Chen and Liu 2000). Both the transmitter and receiver lasers are optically injection-locked from external lasers in the closed-loop system, while only the transmitter laser is injection-locked in the case of the open-loop system. The open-loop system is also a special case of the closed-loop system. In the following, we formulate chaos synchronization in closed-loop systems of optically injected semiconductor lasers.

The optical injection-locking semiconductor laser is a coherent system. Therefore, the model must be described by the rate equations of the field, the phase, and the carrier density

$$\frac{dA_T(t)}{dt} = \frac{1}{2}G_{n,T}\{n_T(t) - n_{th,T}\}A_T(t) + \frac{\kappa_{inj,T}}{\tau_{in,T}}A_{inj,T}(t)\cos\theta_T(t) \quad (12.49)$$

$$\frac{d\phi_T(t)}{dt} = \frac{1}{2}\alpha_T G_{n,T}\{n_T(t) - n_{th,T}\} - \frac{\kappa_{inj,T}}{\tau_{in,T}}\frac{A_{inj,T}(t)}{A_T(t)}\sin\theta_T(t) \quad (12.50)$$

$$\frac{dn_T(t)}{dt} = \frac{J_T}{ed} - \frac{n_T(t)}{\tau_{s,T}} - G_{n,T}\{n_T(t) - n_{0,T}\}A_T^2(t) \quad (12.51)$$

$$\theta_T(t) = -\Delta\omega_T t + \phi_T(t) - \phi_{\text{inj},T}(t) \quad (12.52)$$

The parameters in the above equations are essentially the same as those of previous equations. $\Delta\omega_T$ is the frequency detuning between the transmitter laser and the injection laser. The receiver driven by the transmitted signal can be described by

$$\begin{aligned} \frac{dA_R(t)}{dt} = & \frac{1}{2} G_{n,R} \{n_R(t) - n_{\text{th},R}\} A_R(t) + \frac{\kappa_{\text{inj},R}}{\tau_{\text{in},R}} A_{\text{inj},R}(t) \cos \theta_R(t) \\ & + \frac{\kappa_{\text{cp}}}{\tau_{\text{in},R}} A_T(t - \tau_c) \cos \xi_c(t) \end{aligned} \quad (12.53)$$

$$\begin{aligned} \frac{d\phi_R(t)}{dt} = & \frac{1}{2} \alpha_R G_{n,R} \{n_R(t) - n_{\text{th},R}\} - \frac{\kappa_{\text{inj},R}}{\tau_{\text{in},R}} \frac{A_{\text{inj},R}(t)}{A_R(t)} \sin \theta_R(t) \\ & - \frac{\kappa_{\text{cp}}}{\tau_{\text{in},R}} \frac{A_T(t - \tau_c)}{A_R(t)} \sin \xi_c(t) \end{aligned} \quad (12.54)$$

$$\frac{dn_R(t)}{dt} = \frac{J_R}{ed} - \frac{n_R(t)}{\tau_{s,R}} - G_{n,R} \{n_R(t) - n_{0,R}\} A_R^2(t) \quad (12.55)$$

$$\theta_R(t) = -\Delta\omega_R t + \phi_R(t) - \phi_{\text{inj},R}(t) \quad (12.56)$$

$$\xi_c(t) = \omega_{0,T} \tau_c + \phi_R(t) - \phi_T(t - \tau_c) + \Delta\omega t \quad (12.57)$$

where $\Delta\omega_R$ is the detuning between the receiver and injection lasers, and $\Delta\omega$ is also the detuning between the transmitter and receiver lasers. As can be understood from these equations, chaos synchronization in the systems originates from injection-locking and amplification. Under the special conditions of

$$\frac{1}{\tau_{\text{ph},R}} = \frac{1}{\tau_{\text{ph},T}} \mp \frac{2\alpha\kappa_{\text{cp}}}{\tau_{\text{in},R}\sqrt{1+\alpha^2}} \quad (12.58)$$

$$\omega_{0,T} \tau_c = -\cot^{-1} \alpha \quad (12.59)$$

$$\Delta\omega = 0 \quad (12.60)$$

$$\Delta\omega_R = \Delta\omega_T \quad (12.61)$$

we obtain complete chaos synchronizations (Liu et al. 2001a,b,c)

$$A_R(t) = A_T(t - \tau_c) \quad (12.62)$$

$$\phi_R(t) = \phi_T(t - \tau_c) \quad (12.63)$$

In (12.58), minus sign is for $\sin \omega_{0,T} \tau_c > 0$, while plus sign is for $\sin \omega_{0,T} \tau_c < 0$. We assume without loss of generality that the other parameter values of the two lasers are the same and the phases of the injection lasers, $\phi_{\text{inj},R}(t) = \phi_{\text{inj},T}(t)$, are constant. The condition in (12.58) contains the internal device parameters (τ_{ph} and α) and the external coupling constant. Therefore, it is usually difficult to realize complete chaos synchronization in this system, since the adjustment of the parameters is extremely difficult in real experiments.

12.4.2 Examples of Chaos Synchronization in Injected Lasers

Figure 12.15 shows the experimental results of chaos synchronization using chaotic semiconductor lasers by optical injection (Liu et al. 2001a). The system used is an open-loop system and, therefore, optical injection is only presented in the transmitter system. The frequency detuning between the transmitter and injection lasers is changed to generate various chaotic states. Chaos synchronization is realized at period-1, period-2, and chaotic oscillations. Figure 12.16 plots the numerical results of synchronization errors for the parameter mismatches in the system (Chen and Liu 2000). The figure corresponds to the synchronization errors in complete chaos synchronization. The errors of synchronization are asymmetry for the parameter mismatches, which is similar to the trend for the case of the optical feedback system in Fig. 12.8b. The tolerances for the differential carrier relaxation rate, the nonlinear carrier relaxation rate, and the linewidth enhancement factor are much less effective, but the mismatch of the cavity decay rate $1/\tau_{\text{ph}}$ greatly affects the performance of chaos synchronization. In real devices, we could not easily access and vary the device parameters, therefore we must carefully select lasers with similar characteristics even if the lasers come from the same wafer. It is said that semiconductor laser devices have parameter mismatches within 5–20% in industrial standards. In real lasers, we must also take noise effects into account. Therefore, the coupling coefficient κ_{cp} from the transmitter to the receiver lasers must be larger than a certain value to take on a negative value for the conditional Lyapunov exponent.

12.5 Chaos Synchronization in Optoelectronic Feedback Systems

12.5.1 Theory of Chaos Synchronization in Optoelectronic Feedback Systems

We discussed chaotic oscillations in optoelectronic feedback in semiconductor lasers in Chap. 7. We here assume the chaotic generators of optoelectronic feedback lasers depicted in Fig. 7.1. In optoelectronic feedback systems, the rate equations for the

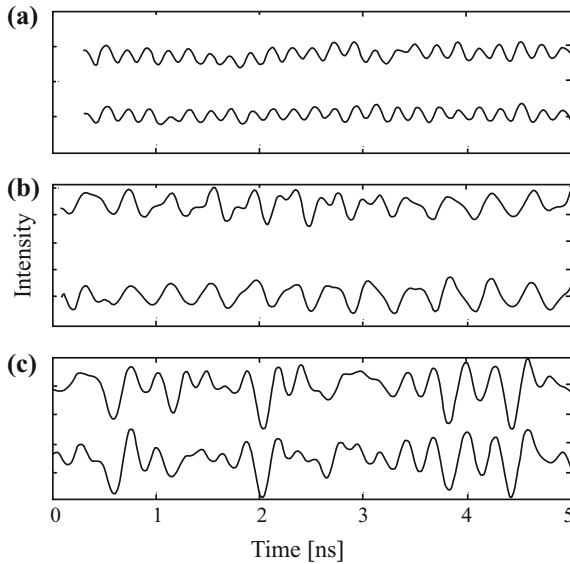


Fig. 12.15 Experimental chaos synchronization using chaotic semiconductor lasers by optical injection. The system is an open-loop. The frequency detuning between the transmitter and injection lasers is changed to generate various chaotic states at a fixed injection rate. Synchronized waveforms at **a** period-1, **b** period-2, and **c** chaotic oscillations. In each figure, the *upper trace* is the transmitter output and the *lower trace* is the receiver output. The lasers used are DFB lasers with an oscillation wavelength of $1.3\mu\text{m}$. The chaos synchronization is achieved under the complete condition [after Liu et al. (2001a); © 2001 IEEE]

photon number and the carrier density are enough for describing the systems. Optoelectronic feedback systems in semiconductor lasers have an advantage of excellent synchronization performance over optical feedback and optical injection systems. Since the time scale for the carrier density is three figures larger than that of the photon lifetime, the performance, and accuracy of chaos synchronization in optoelectronic feedback systems are different from those of optical feedback and optical injection systems. The points will be again discussed in the next chapter from the viewpoint of data transmission capability in chaotic communications. The rate equations for the photon number and the carrier density in a transmitter of optoelectronic feedback are written by

$$\frac{dS_T(t)}{dt} = G_{n,T}\{n_T(t) - n_{th,T}\}S_T(t) + R_{sp,T} \quad (12.64)$$

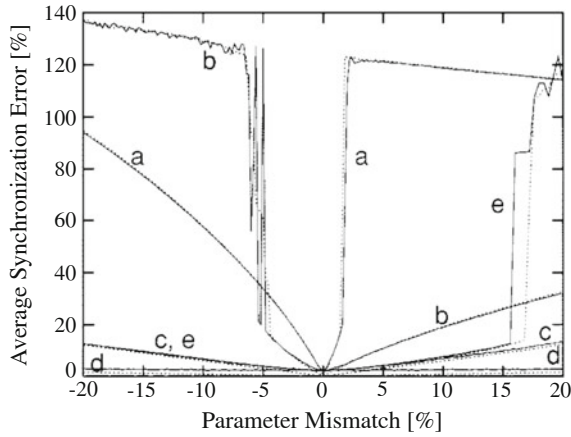


Fig. 12.16 Synchronization error (%) versus parameter mismatch (%). Solid curves **a**, **b**, **c**, **d**, and **e** correspond to parameters of cavity decay rate, spontaneous carrier decay rate, differential carrier relaxation rate, nonlinear carrier relaxation rate, and linewidth enhancement factor, respectively. The intrinsic Langevin noise is considered in the simulation. Each corresponding dotted curve is obtained without including the intrinsic noise [after Chen and Liu (2000); © 2000 IEEE]

$$\begin{aligned} \frac{dn_T(t)}{dt} &= \frac{J_T}{ed} \{1 + \xi_T S_T(t - \tau_T)\} \\ &\quad - \frac{n_T(t)}{\tau_{s,T}} - G_{n,T} \{n_T(t) - n_{0,T}\} S_T(t) \end{aligned} \quad (12.65)$$

where ξ_T is the coefficient of the optoelectronic feedback circuit in the transmitter. The rate equations for the receiver laser are given by

$$\frac{dS_R(t)}{dt} = G_{n,R} \{n_R(t) - n_{th,R}\} S_R(t) + R_{sp,R} \quad (12.66)$$

$$\begin{aligned} \frac{dn_R(t)}{dt} &= \frac{J_R}{ed} \{1 + \xi_R S_R(t - \tau_R) + \xi_{cp} S_T(t - \tau_c)\} \\ &\quad - \frac{n_R(t)}{\tau_{s,R}} - G_{n,R} \{n_R(t) - n_{0,R}\} S_R(t) \end{aligned} \quad (12.67)$$

where ξ_R is the coefficient of the optoelectronic feedback circuit in the receiver and ξ_{cp} is the coupling coefficient from the transmitter to the receiver lasers. As discussed in Chap. 7, when the electronic feedback circuit has a finite time response, the feedback terms $s(t) = \xi_T S_T(t - \tau_T)$ and $s(t) = \xi_R S_R(t - \tau_R) + \xi_{cp} S_T(t - \tau_c)$ are replaced by the following integral equation:

$$y(t) = \int_{-\infty}^t f(t' - t)s(t')dt' \quad (12.68)$$

where $f(t)$ is the response function of the electronic circuit. The optoelectronic feedback system is also a delay differential system like the optical feedback system. However, the optoelectronic feedback system is quite different from optical feedback and optical injection systems. For example, the chaotic output from optoelectronic feedback is generally irregular pulsing states. The driving signal to the laser in the optoelectronic feedback system is also a chaotic signal, but the signal is not linearly proportional to the optical output power (Liu et al. 2001b). Chaos synchronization in optoelectronic feedback is generally a complete type (Tang et al. 2001).

12.5.2 Examples of Chaos Synchronization in Optoelectronic Feedback Systems

Figure 12.17 shows the results of chaos synchronization in an open-loop optoelectronic feedback system (Tang et al. 2001). As discussed in Chap. 7, the typical feature of chaotic oscillations in optoelectronic feedback systems is periodic or irregular pulsations of the laser output power. In the figure, chaos synchronization is achieved for various states of chaotic oscillations by changing the feedback time τ_T in the electronic feedback circuit. The synchronization scheme is complete chaos synchronization. Figure 12.18 shows the numerical simulation for the model. Figure 12.18a is the bifurcation diagram for the normalized delay time $\hat{\tau} = \tau \nu_R$ in the transmitter laser. Figure 12.18b is the maximum conditional Lyapunov exponent. Here, the parameter c_p is defined by

$$c_p = 1 - \frac{\xi_R}{\xi_T + \xi_{cp}} \quad (12.69)$$

When the system is a closed-loop, $c_p = 0$, while $c_p = 1$ for an open-loop. From this figure, the maximum conditional Lyapunov exponent in the open-loop system is smaller than that of the closed-loop system. Therefore, the open-loop system can achieve stable chaos synchronization compared with the closed-loop system. The effects of parameter mismatches for chaos synchronization have also been studied in optoelectronic feedback systems and similar results as for optical feedback systems are obtained (Abarbanel et al. 2001).

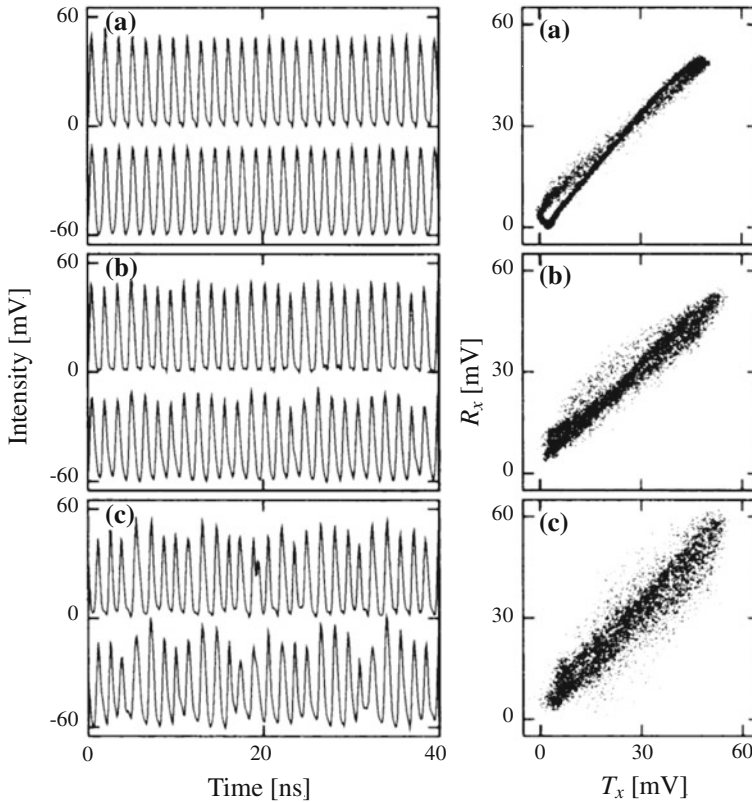
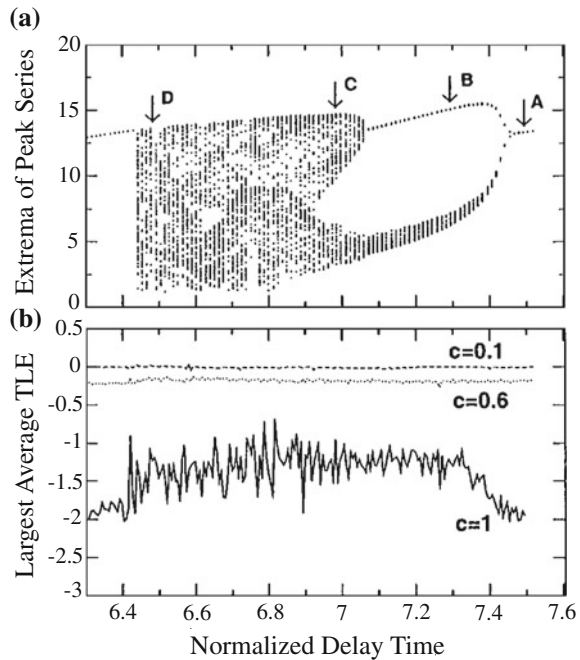


Fig. 12.17 Time series and correlation plots of synchronization at three different pulsing states under $c_p = 1$. **a** Regular pulsing at $\tau = 7.47$ ns, **b** two-frequency quasi-periodic pulsing at $\tau = 7.09$ ns, **c** chaotic pulsing at $\tau = 6.92$ ns. In **a–c** the *upper trace* is for the transmitter and the *lower trace* is for the receiver. The *left row* is the time series and the *right row* is the correlation plots. The laser is a DFB laser with the oscillation wavelength at $1.30 \mu\text{m}$. The relaxation oscillation frequency of the laser is 2.5 GHz at the operating condition [after Tang et al. (2001); © 2001 OSA]

12.6 Chaos Synchronization in Injection Current Modulated Systems

Semiconductor lasers are sensitive to injection current modulation and sometimes show chaotic oscillations for certain conditions both of the device parameters and the modulation frequency and index as discussed in Chaps. 6 and 7. However, chaotic oscillations by the frequency modulation occur only under limited conditions in ordinary narrow-stripe edge-emitting semiconductor lasers. Therefore, we briefly introduce a chaos synchronization system using a frequency modulated self-pulsating semiconductor laser as a chaotic light source. The output from a self-pulsating semiconductor laser shows regular pulsating oscillations for the ideal case. The laser is

Fig. 12.18 Conditions for stable route-tracking synchronization. **a** Bifurcation diagram. *A*: regular pulsing, *B*: two-frequency quasi-periodic pulsing, *C*: three-frequency quasi-periodic pulsing, *D*: chaotic pulsing. **b** Largest average conditional Lyapunov exponent (transverse Lyapunov exponent) of coupled system for the same dynamic states as in **a** under different coupling strengths, $c_p = 0.1, 0.6,$ and 1 [after Tang et al. (2001); © 2001 OSA]



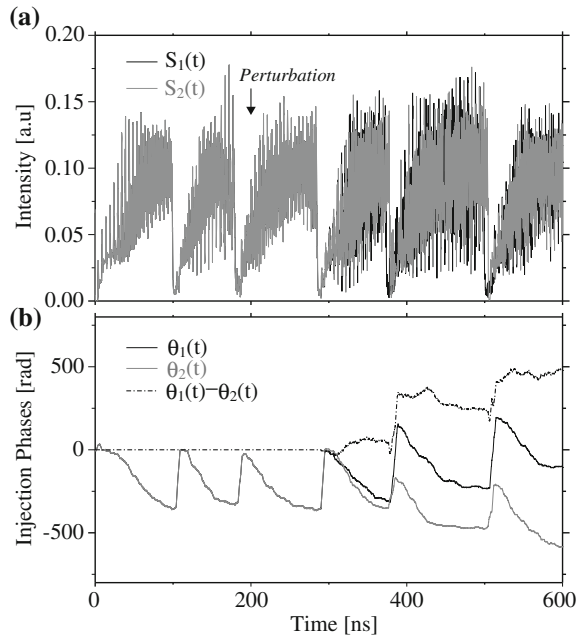
used as a light source of a digital versatile disk system. However, the laser easily exhibits chaotic oscillations (irregular pulsing states) under an appropriate combination of the modulation frequency and index for the bias injection current as discussed in Sect. 8.2. In the chaotic oscillations, pulse heights of the pulsating output irregularly fluctuate and this fluctuation is proved to be chaotic. Jones et al. (2001) demonstrated numerically chaos synchronization in symmetrical modulation systems. They used a very high frequency modulation of 3.4 GHz with a large modulation index of 0.3. Their model was a coherent coupling between the transmitter and receiver lasers. However, incoherent coupling must be taken into account through a long transmission line between the transmitter and receiver systems, since a self-pulsating semiconductor laser has once brought almost below the laser threshold after a pulsation. Only a few studies have been published on chaos synchronization in modulated semiconductor lasers to date.

12.7 Chaos Synchronization in Mutually Coupled Lasers

12.7.1 Mutually Coupled Edge-Emitting Semiconductor Lasers

Mutually coupled oscillators are of great interest because of the important insight they provide into coupled physical, chemical, and biological systems. Mutually coupled

Fig. 12.19 Numerical simulation describing the transition phenomenon from the isochronal to achronal solution due to perturbations of Langevin noises applied at $t = 200$ ns. **a** Intensity time traces and **b** the dynamics of the injection phases. The parameters are $\tau_c = 5$ ns, $\kappa_{cp}/\tau_{in} = 20$ ns⁻¹, and $J/J_{th} = 1$ [after Mulet et al. (2004); © 2004 IOP]



semiconductor lasers can be used for a system of chaos synchronization. However, the dynamics have not been fully studied in semiconductor lasers, since the straightforward applications of the systems such as for secure communications are not easy. Example of chaotic secure communications based on mutual coupling systems is treated in Chap. 13. In this subsection, we concern chaos synchronization in mutually coupled narrow-stripe edge-emitting semiconductor lasers (Hohl et al. 1997, 1999; Heil et al. 2001; Mirasso et al. 2002; Mulet et al. 2002, 2004; Klein et al. 2006). In an unbalanced mutual coupling system, (for example, frequency detuned system or parameter mismatched system), one of the lasers become the leader and the other is the lagger as concerning to their time series as discussed in Sect. 12.2.5. In accordance with the discussion in Sect. 12.2.5, chaos synchronization originated by injection-locking phenomena can be studied and the detail of the conditions for chaos synchronization in leader-lagger configurations of chaotic waveforms is found in literature (Heil et al. 2001). Here, we focus on the transition phenomenon of chaos synchronization in an intrinsically complete configuration. As mentioned in Sect. 12.2.5, an isochronal solution in the mutual coupling semiconductor lasers is easily transitioned to an achronal state due to the presence of noises in spite of highly symmetrical conditions.

Figure 12.19 shows a numerical example of transitions from complete to generalized chaos synchronization in a symmetrical system of mutual coupling semiconductor lasers (Mulet et al. 2004). In the numerical simulation, the coupled two lasers without optical feedback have the same device parameters and driving conditions. In

Fig. 12.19a, the time traces of the two lasers at first output completely the same waveforms, since the rate equations do not include the noise terms. However, the output powers deviate with each other and the synchronization is transitioned to achronal state from complete isochronal one after the noises are switched on at $t = 200$ ns. Since the lasers are biased at low current $J/J_{\text{th}} = 1$, the output powers show LFFs. Figure 12.19b shows the dynamics of the phases (θ_1 and θ_2 in (12.25) and (12.29)) and their difference. Before the perturbation is applied, the two phases completely show identical traces. However, after one transient LFF following the perturbation, the two phase traces deviate with each other. In the situation of a highly symmetrical mutual coupling system, which laser becomes the leader or lagger is determined by statistically. Further, the leader is once switched to the lagger and at the other occasion it returns to the leader. The process is described by the statistical potential model, which has already discussed in Sect. 5.1.2, and the transition is kicked by the Langevin noises. To show the physical effects clearly, the case for a low bias injection current is shown in Fig. 12.19. However, similar phenomena are also observed at higher bias injection current with fast chaotic oscillations whose main frequency component corresponds to the laser relaxation oscillation. We cannot avoid statistical noises in real semiconductor lasers, so that we only observe leader and lagger chaotic signals in experimental mutual coupling systems with symmetrical configuration, even if the two coupling lasers are carefully prepared to take the same characteristics. It is noted that such instability of the switching between leader and lagger configurations occurs only for symmetrical systems. When an asymmetry is introduced for a synchronization system of mutual coupling semiconductor lasers with optical feedback, we obtain a fixed relation of the time lag between the laser outputs even for complete chaos synchronization scheme as will be discussed in Sect. 13.5. Synchronization is also attained in polarization-rotated mutual coupling systems and synchronous oscillations of square-wave forms between two lasers have been demonstrated (Sukow et al. 2010). Oscillations of square-wave forms and anti-phase synchronization are typical features in semiconductor lasers with polarization-rotated optical feedback as discussed in Sect. 5.8.2. The tolerances for the parameter mismatches in mutually coupled narrow-stripe edge-emitting semiconductor lasers have also been discussed (Avila and Leite 2009; Hicke et al. 2011).

12.7.2 Mutually Coupled VCSELs

Several reports have also been published for chaos synchronization with mutually coupled VCSELs (Spencer et al. 1998; Spencer and Mirasso 1999; Fujino and Ohtsubo 2001). In mutually coupled VCSELs, two orthogonal polarization modes are simultaneously excited and the polarization dynamics must be taken into account. We here show chaos synchronization in mutually coupled VCSELs in LFF regimes (Fujiwara et al. 2003). In the experiments, mutually coupled VCSELs without external mirrors are used. Even when the lasers are stable at the free running state, they exhibit chaotic oscillations under mutual coupling. Figure 12.20 shows the results of

chaos synchronization. Figure 12.20a plots time series and their optical spectra of the x -polarization components of the two lasers at LFF oscillations. Figure 12.20b shows the results for the y -polarization components. The lasers are biased at low injection currents and their spatial modes are the lowest ones, i.e., LP_{01} mode. In the experiment, the two polarization modes are mutually coupled with each other. In this example, chaos synchronization occurs by the coupling with the x -polarization components and one of the outputs of the orthogonal y -polarization components synchronizes to the other under the anti-correlation effect. This fact is easily understood from the observation of optical spectra in the figure. Anti-phase correlation of the two orthogonal polarization components is a typical feature in VCSELs. At the solitary oscillations, the y -polarization modes are dominant lasing modes and the laser powers are almost concentrated to the y -polarization modes. On the other hand, the x -polarization modes increase and become the dominant modes after the mutual coupling. The laser oscillation of VCSEL2 lags with respect to VCSEL1 with 4 ns (the transmission time of light from one laser to the other), therefore the synchronization is a generalized case. Fujiwara and Ohtsubo (2004) also showed chaos synchronization for a selective polarization mode in mutually coupled VCSELs. Though the other mode is not coupled, the remaining modes synchronize with the anti-phase correlation effect. Chaos synchronization in VCSELs occurs even for the two different spatial modes as far as detuning of the oscillation frequencies is negligibly small.

12.7.3 Optoelectronic Mutually Coupled Semiconductor Lasers

The dynamics and chaos synchronization for mutually coupled systems in semiconductor lasers with optoelectronic feedback was studied by Tang et al. (2004). In the system, mutual coupling can act as a negative feedback to stabilize the coupled oscillators or it can increase the complexity of the system inducing a highly complex chaos depending on the operating conditions. A quasi-periodicity and period-doubling bifurcation, or a mixture of the two, is found in such a system. Also, the system exhibits a unique state of stabilizing and quenching the oscillation amplitude of two pulsating oscillators, a phenomenon known as “death by delay”. Although the chaotic waveforms are very complex with broad spectra, a high quality of synchronization between the chaotic waveforms is observed. Such synchronization is achieved because of the effect of mutual coupling and the symmetric design between the two lasers. Figure 12.21 shows a schematic diagram for semiconductor lasers with mutual optoelectronic coupling. The fundamental chaotic oscillator is the same as the system of optoelectronic feedback as discussed in Sect. 12.5.1. A part of an emitted light from semiconductor laser LD 1 is once detected by photodetector PD 1 and electronically fed back into the bias injection current of the laser with delay τ_1 . On the other hand, the other light is detected by photodetector PD 2 and fed into the bias injection current of semiconductor laser LD 2 with transmission time T_1 . Similarly, semiconductor laser LD 2 also has an optoelectronic feedback loop with

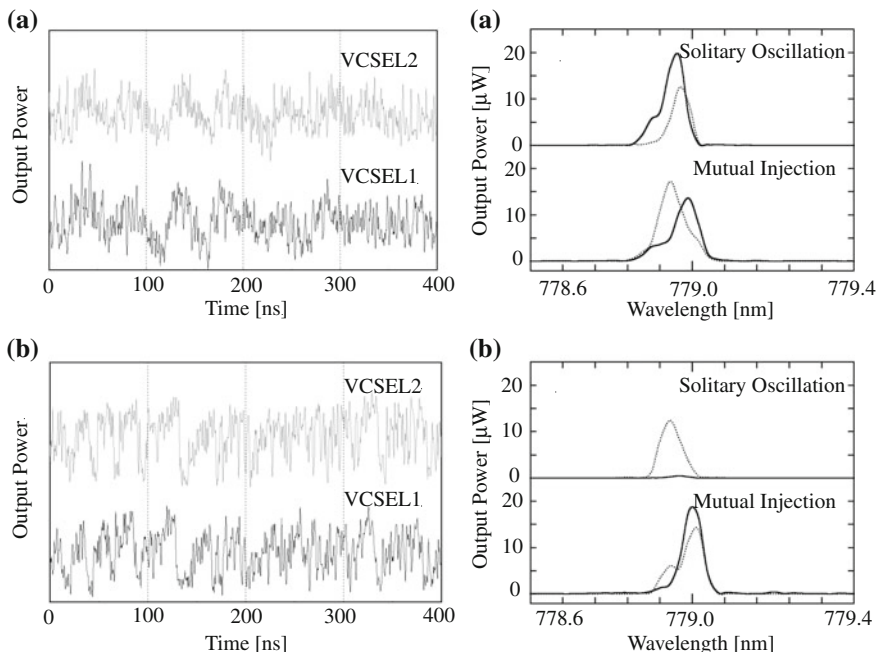


Fig. 12.20 Chaos synchronization in mutually coupled VCSELs in an LFF regime. **a** *x*-polarization mode and **b** *y*-polarization mode. The *left* is the time series and the *right* is the corresponding optical spectra. *Solid curves*: VCSEL 1, *dotted curves*: VCSEL2. The coupling time of light between the two lasers is 4 ns

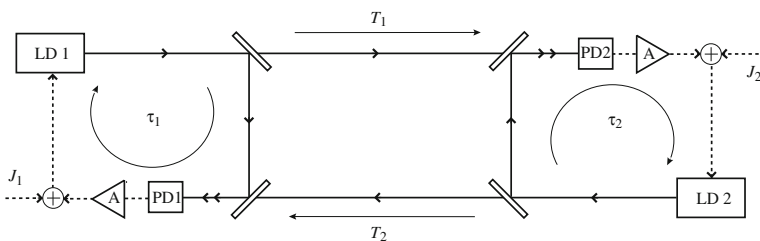


Fig. 12.21 Schematic diagram of mutually coupled semiconductor lasers with optoelectronic feedback. LD: laser diode, PD: photodiode, A: amplifier, I: bias injection current

time delay τ_2 . A part of an emitted light from the laser LD 2 is also fed into the first laser with transmission time T_2 , thus mutual coupling of the system is attained.

The system of the mutual coupling lasers can be easily described by extending the discussion in Sect. 12.5. For semiconductor laser LD 1, one reads

$$\frac{dS_1(t)}{dt} = [G_{n1}\{n_1(t) - n_{th1}\}]S_1(t) \tag{12.70}$$

$$\begin{aligned} \frac{dn_1(t)}{dt} = & \frac{J_1(t)}{ed} \{1 + \xi_{f1} S_1(t - \tau_1) + \xi_{cp1} S_2(t - T_2)\} \\ & - \frac{n_1(t)}{\tau_{s1}} - G_{n1} \{n_1(t) - n_{01}\} S_1(t) \end{aligned} \quad (12.71)$$

Here, we assume an instantaneous response of the electronic feedback circuit, however, we can apply (12.68) for a finite response of the circuit. For the second laser, the coupling equations can be written as symmetric forms as above equations by

$$\frac{dS_2(t)}{dt} = [G_{n2} \{n_2(t) - n_{th2}\}] S_2(t) \quad (12.72)$$

$$\begin{aligned} \frac{dn_2(t)}{dt} = & \frac{J_2(t)}{ed} \{1 + \xi_{f2} S_2(t - \tau_2) + \xi_{cp2} S_1(t - T_1)\} \\ & - \frac{n_2(t)}{\tau_{s2}} - G_{n2} \{n_2(t) - n_{02}\} S_2(t) \end{aligned} \quad (12.73)$$

In mutually coupled semiconductor lasers, not only that the output of one laser is coupled into the dynamics of the other laser, but also that the time delay introduced by the mutual coupling further increases the dimension of the degree of freedom in the coupled lasers. Consequently, a lot of interesting dynamics have been observed in such mutually coupled semiconductor lasers. For example, optoelectronic feedback can drive semiconductor lasers into nonlinear oscillations, such as regular pulsing, quasi-periodic pulsing, or chaotic pulsing under certain conditions of the device and feedback parameters. One of typical features in this system is a death by delay, in which two limit-cycle oscillators suddenly stop oscillating due to a time-delayed coupling between these oscillators by tuning the feedback parameters (Tang et al. 2004). The phenomenon of death by delay has been observed in many other mutually coupled limit-cycle oscillators, which do not necessarily have a delayed feedback. In the mutually coupled optoelectronic feedback systems described by (12.70)–(12.73), we can observe periodic death islands of the laser oscillations at a certain coupling strength for the increase of the coupling delay time $T_1 + T_2$. In reality, there is always a bandwidth limitation from the components such as the amplifiers, the photodetectors, and even the lasers. Consequently, the mutually coupled semiconductor laser system is not only highly nonlinear but also highly dispersive. The system can have a quasi-periodic pulsing route, a period-doubling pulsing route, or a mixture of these two bifurcations to chaos. The system has very interesting properties as a viewpoint of nonlinear dynamics. However, we here focus on the synchronization properties of the system.

Experimental and theoretical studies for synchronization of mutually coupled semiconductor lasers with optoelectronic feedback were reported by Tang et al. (2004) and Chiang et al. (2005). The two semiconductor lasers are operated in states of regular oscillations or quasi-periodic oscillations under the effect of optoelectronic feedback before the mutual coupling is applied. Once the mutual coupling is applied,

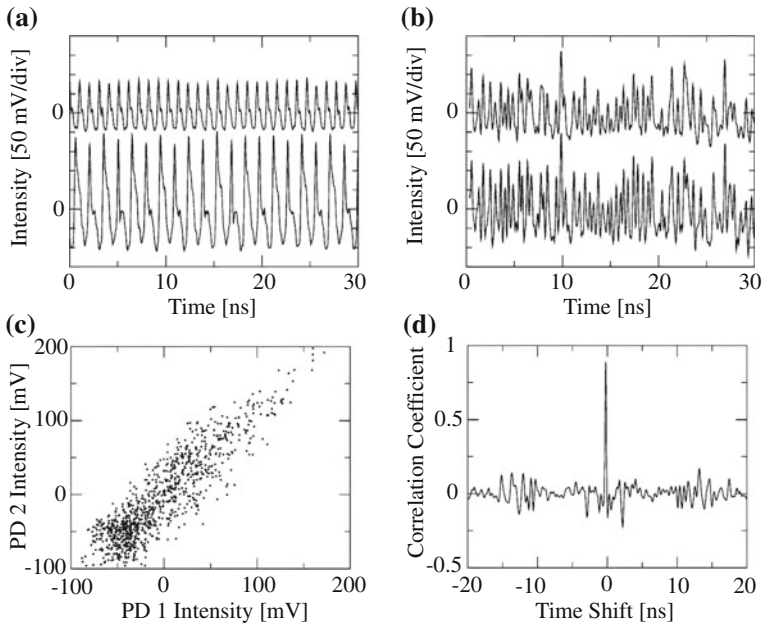


Fig. 12.22 Experimental chaos synchronization in semiconductor lasers with mutual optoelectronic coupling. $T_1 = T_2 = 15.4$ ns and $\tau_1 = \tau_2 = 5.4$ ns. **a** Time series of regular pulsing states in the two lasers before mutual coupling. **b** Chaotic time series after mutual coupling. **c** and **d** Correlation plot of the photodiode outputs after mutual coupling [after Tang et al. (2004); © 2004 IEEE]

dramatic effects can be observed on the original nonlinear oscillations. Figure 12.22 shows an experimental example of chaos synchronization in this system. Without mutual coupling, the waveforms from the two lasers may exhibit either typical pulsing states or chaotic pulsing states at certain oscillation conditions. In this case, the waveform from PD 1 is a regular pulsing state with one fundamental frequency, while that from PD 2 is a quasi-periodic pulsing state as shown in Fig. 12.22a. With mutual coupling, highly complex chaotic outputs from the two lasers are observed under the conditions of $T_1 = T_2 = \tau_1 = \tau_2 = 15.4$ ns as shown in Fig. 12.22b. It is noted that the two waveforms have a zero time lag and the type of synchronization is complete. Figure 12.22c and d show the correlation plot between the outputs from PD 1 and PD 2, and the time shifted correlation, respectively. The detailed properties of chaos synchronization in mutually coupled semiconductor lasers with optoelectronic feedback were reported in the references (Chiang et al. 2005, 2006).

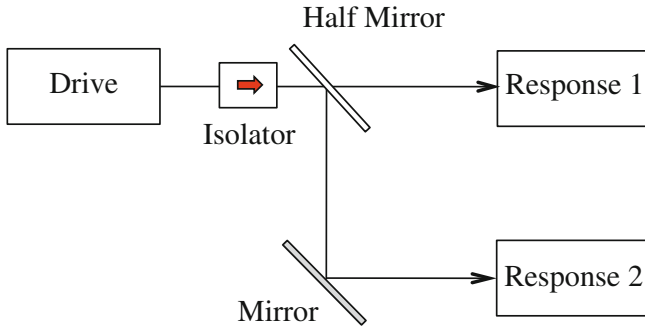


Fig. 12.23 Drive and response configuration in chaos synchronization system. Two response laser are injected by chaotic light from the drive laser

12.8 Common-Chaotic-Signal Induced Synchronization in Semiconductor Lasers

In the preceding sections, we discussed chaos synchronization with two coupled lasers, either in unidirectionally or mutually coupled configuration. However, we can introduce a third chaotic laser in the systems of chaos synchronization. In this configuration, transmitter and receiver lasers are simultaneously injected by the same chaotic signal from the third drive laser and, thus, the accuracy of chaos synchronization between the transmitter and receiver lasers is greatly enhanced. For example, we prepare three chaotic systems consisting of semiconductor lasers with optical feedback; one is assigned to the driving system and the others are used for the response systems. Then, the output from the drive unidirectionally injects the response lasers (Yamamoto et al. 2007; Oowada et al. 2009). The other instance is a mutual coupling system with a third driving laser. In this system, in-between transmitter and receiver lasers, the third laser is introduced as a buffer of the chaotic signal transmissions (Fischer et al. 2006; Vicente et al. 2008). In both cases, we can obtain higher correlations between the transmitter and receiver chaotic signals compared with common two-laser synchronization systems. Figure 12.23 shows a system for the first case. Any chaotic systems may be used as a drive and responses, however, we here assume optical feedback systems of semiconductor lasers for all three systems. The response systems may not be the same characteristics to the drive system; however, the two response systems are required to have closely similar characteristics with each other not only for the device characteristics but also for the operation conditions. The output powers from response 1 and response 2 show similar chaotic oscillations by the injection of a chaotic signal from the drive system. The driving chaotic signal and the synchronous response signals may not have good correlations, since the adjustment of the parameters between the drive and the responses are rather loose. However, we can obtain a good correlation between the two response systems. The phenomena are confirmed not only by experiments but also by numerical simulations.

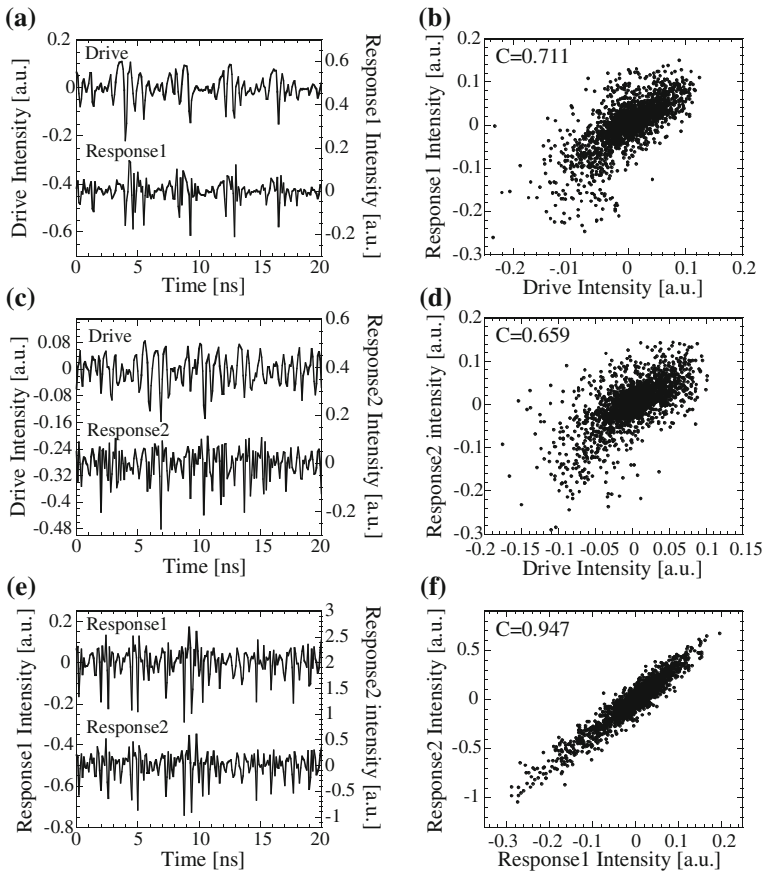


Fig. 12.24 Experimental result of temporal waveforms and corresponding correlation plots for **a, b** Drive and Response 1, **c, d** Drive and Response 2, and **e, f** Response 1 and Response 2. The coupling delay time (4.0 ns) between the two temporal waveforms is compensated in **a–d**. The cross correlation values are **b** 0.711, **d** 0.659, and **f** 0.947 [after Yamamoto et al. (2007); © 2007 OSA]

Figure 12.24 shows an experimental example of chaos synchronization in drive-response systems. In this case, the driving system is a semiconductor laser with optical feedback (feedback delay time of 4 ns), however, the response systems are solitary semiconductor lasers without optical feedback. The three lasers are all the same DFB lasers with oscillation wavelength of $1.55 \mu\text{m}$, which come from the same wafer. At the operation conditions, the response lasers have the same optical wavelength of 1547.356 nm , while the drive laser is biased at lower current and its oscillation wavelength is 1547.376 nm (the corresponding frequency detuning between the drive and response lasers is -2.5 GHz). Since the frequency detuning is not large, the response lasers are injection-locked to the drive laser and they oscillate similar chaotic signal to the drive laser. Figure 12.24a–d are the results of chaos synchronization. The coupling delay time between the two temporal waveforms is compensated in the time

traces in Fig. 12.24a and c. As is seen from these figures, the response lasers shows similar chaotic waveforms to the response laser, however, the correlation is not so high as around 0.7. On the other hand, the correlation between the response lasers has a high correlation as much as 0.947. In ordinary chaos synchronization systems with two unidirectionally coupled semiconductor lasers, the good correlation values from 0.8 to 0.9 are usually obtained by experiments as far as the synchronization is originated from the effects of optical injection-locking and amplification. Taking the facts into consideration, we can much enhance the correlation of chaos synchronization by the introduction of the third chaotic laser. Although the effects are demonstrated by experiments and corresponding numerical simulations, the mechanism of the enhancement is not fully understood yet.

References

- Abarbanel HDI, Kennel MB, Illing L, Tang S, Chen HF, Liu JM (2001) Synchronization and communication using semiconductor lasers with optoelectronic feedback. *IEEE J Quantum Electron* 37:1301–1311
- Ahlers V, Parlitz U, Lauterborn W (1998) Hyperchaotic dynamics and synchronization of external-cavity semiconductor lasers. *Phys Rev E* 58:7208–7213
- Annovazzi-Lodi V, Donati S, Scirè A (1996) Synchronization of chaotic injected-laser systems and its application to optical cryptography. *IEEE J Quantum Electron* 32:953–959
- Avila JFM, Leite JRR (2009) Time delays in the synchronization of chaotic coupled lasers with feedback. *Opt Express* 24:21442–214451
- Chen HF, Liu JM (2000) Open-loop chaotic synchronization of injection-locked semiconductor lasers with gigahertz range modulation. *IEEE J Quantum Electron* 36:27–34
- Chiang MC, Chen HF, Liu JM (2005) Experimental synchronization of mutually coupled semiconductor lasers with optoelectronic feedback. *IEEE J Quantum Electron* 41:1333–1340
- Chiang M, Chen HF, Liu JM (2006) Synchronization of mutually coupled systems. *Opt Commun* 261:86–90
- Cuomo KM, Oppenheim AV, Stogatz SH (1993) Synchronization of Lorenz-based chaotic circuits with applications to communications. *IEEE Trans Circuits Syst II* 40:626–633
- Fischer I, Liu Y, Davis P (2000a) Synchronization of chaotic semiconductor laser dynamics on subnanosecond time scales and its potential for chaos communication. *Phys Rev A* 62: 011801-1–4
- Fischer APA, Andersen OK, Yousefi M, Stolte S, Lenstra D (2000b) Experimental and theoretical study of filtered optical feedback in a semiconductor laser. *IEEE J Quantum Electron* 36:375–384
- Fischer I, Vicente R, Buldú JM, Peil M, Mirasso CR, Torrent MC, Garcíá-Ojalvo J (2006) Zero-lag long-range synchronization via dynamical relaying. *Phys Rev Lett* 97: 123902-1–4
- Fujino H, Ohtsubo J (2000) Experimental synchronization of chaotic oscillations in external cavity semiconductor lasers. *Opt Lett* 25:625–627
- Fujino H, Ohtsubo J (2001) Synchronization of chaotic oscillations in mutually coupled semiconductor lasers. *Opt Rev* 8:351–357
- Fujiwara N, Takiguchi Y, Ohtsubo J (2003) Observation of the synchronization of chaos in mutually injected vertical-cavity surface-emitting semiconductor lasers. *Opt Lett* 28:1677–1679
- Fujiwara N, Ohtsubo J (2004) Synchronization in chaotic vertical-cavity surface-emitting semiconductor lasers. *SPIE Proc* 5349:282–289

- Garcia-Ojalvo J, Casademont J, Mirasso CR, Torrent MC, Sancho JM (1999) Coherence and synchronization in diode-laser arrays with delayed global coupling. *Int J of Bifurcat and Chaos* 9:2225–2229
- Heil T, Fischer I, Elsässer W, Mulet J, Mirasso CR (2001) Chaos synchronization and spontaneous symmetry breaking in symmetrical delay-coupled semiconductor lasers. *Phys Rev Lett* 86:795–798
- Hicke K, D’Huys O, Flunkert V, E. Schöll E, Danckaert J, Fischer I (2011) Mismatch and synchronization: Influence of asymmetries in systems of two delay-coupled lasers. *Phys Rev E* 83: 056211-1–11
- Hohl A, Gavrielides A, Erneux T, Kovanis V (1997) Localized synchronization in two coupled nonidentical semiconductor lasers. *Phys Rev Lett* 78:4745–4748
- Hohl A, Gavrielides A, Erneux T, Kovanis V (1999) Quasiperiodic synchronization for two delay-coupled semiconductor lasers. *Phys Rev A* 59:3941–3949
- Jones RJ, Rees P, Spencer PS, Shore KA (2001) Chaos and synchronization of self-pulsating laser diodes. *J Opt Soc Am B* 18:166–172
- Klein E, Gross N, Rosenbluh M, Kinze W, Khaykovich L, Kanter I (2006) Stable isochronal synchronization of mutually coupled chaotic lasers. *Phys Rev E* 73: 066214-1–4
- Kusumoto K, Ohtsubo J (2003) Anticipating chaos synchronization at high optical feedback rate in compound cavity semiconductor lasers. *IEEE J Quantum Electron* 39:1531–1536
- Liu Y, Davis P (2000) Dual synchronization of chaos. *Phys Rev E* 61:R2176–2179
- Liu Y, Davis P (2001) Synchronized chaotic mode hopping in DBR lasers with delayed opto-electric feedback. *IEEE J Quantum Electron* 37:337–352
- Liu JM, Chen HF, Tang S (2001a) Optical-communication systems based on chaos in semiconductor lasers. *IEEE Trans Circuits Syst I* 48:1475–1483
- Liu JM, Chen HF, Tang S (2001b) Synchronization of chaos in semiconductor lasers. *Nonlinear Anal* 47:5741–5751
- Liu Y, Chen HF, Liu JM, Davis P, Aida T (2001c) Communication using synchronization of optical-feedback-induced chaos in semiconductor lasers. *IEEE Trans Circuits Syst I* 48:1484–1490
- Liu Y, Takiguchi Y, Davis P, Aida T, Saito S, Liu JM (2002) Experimental observation of complete chaos synchronization in semiconductor lasers. *Appl Phys Lett* 80:4306–4308
- Masoller C (2001) Anticipation in the synchronization of chaotic semiconductor lasers with optical feedback. *Phys Rev Lett* 86:2782–2785
- Mirasso CR, Kolesik M, Matus M, White JK, Moloney JV (2002) Synchronization and multimode dynamics of mutually coupled semiconductor lasers. *Phys Rev A* 65: 013805-1–4
- Mirasso CR, van Tartwijk GHM, Hernández-García E, Lenstra D, Lynch S, Landais P, Phelan P, O’Gorman J, Elsässer W (1999) Self-pulsating semiconductor lasers: theory and experiment. *IEEE J Quantum Electron* 35:764–770
- Mulet J, Masoller C, Mirasso CR (2002) Modeling bidirectionally coupled single-mode semiconductor lasers. *Phys Rev A* 65: 063815-1–12
- Mulet J, Mirasso CR, Heil T, Fischer I (2004) Synchronization scenario of two distant mutually coupled semiconductor lasers. *J Opt B Quantum Semiclassical Opt* 6:97–105
- Murakami A, Ohtsubo J (2002) Synchronization of feedback-induced chaos in semiconductor lasers by optical injection. *Phys Rev A* 65: 033826-1–7
- Ohtsubo J (2002a) Chaotic dynamics in semiconductor lasers with optical feedback. In: Wolf E (ed) *Progress in optics*, Chap. 1, Vol 44, North-Holland, Amsterdam
- Ohtsubo J (2002b) Chaos synchronization and chaotic signal masking in semiconductor lasers with optical feedback. *IEEE J Quantum Electron* 38:1141–1154
- Oowada I, Ariizumi H, Li M, Yoshimori S, Uchida A, Yoshimura K, Davis P (2009) Synchronization by injection of common chaotic signal in semiconductor lasers with optical feedback. *Opt Express* 17:10025–10034
- Pecora LM, Carroll TL (1990) Synchronization in chaotic systems. *Phys Rev Lett* 64:821–824
- Pecora LM, Carroll TL (1991) Driving systems with chaotic signals. *Phys Rev Lett* 44:2374–2384

- Peters-Flynn S, Spencer PS, Sivaprakasam S, Pierce I, Shore KA (2006) Identification of the optimum time-delay for chaos synchronization regimes of semiconductor lasers. *IEEE J Quantum Electron* 42:427–434
- Rogister F, Locquet A, Pieroux D, Sciamanna M, Deparis O, Megret P, Blondel M (2001) Secure communication scheme using chaotic laser diodes subject to incoherent optical feedback and incoherent optical injection. *Opt Lett* 26:1466–1469
- Roy R, Thornburg KS Jr (1994) Experimental synchronization of chaotic lasers. *Phy Rev Lett* 72:2009–2015
- Sauer M, Kaiser F (1998) On-off intermittency and bubbling in the synchronization break-down of coupled lasers. *Phys Lett A* 243:38–46
- Shibasaki N, Uchida A, Yoshimori Y, Davis P (2006) Characteristics of chaos synchronization in semiconductor lasers subject to polarization-rotated optical feedback. *IEEE J Quantum Electron* 42:342–350
- Sivaprakasam S, Shahverdiev EM, Spencer PS, Shore KA (2001) Experimental demonstration of anticipating synchronization in chaotic semiconductor lasers with optical feedback. *Phys Rev Lett* 87: 154101-1–3
- Sivaprakasam S, Shahverdiev EM, Shore KA (2000) Experimental verification of the synchronization condition for chaotic external cavity diode lasers. *Phys Rev E* 62:7505–7507
- Someya H, Oowada I, Okumura H, Kida T, Uchida A (2009) Synchronization of bandwidth-enhanced chaos in semiconductor lasers with optical feedback and injection. *Opt Express* 17:19536–19543
- Spencer PS, Mirasso CR, Colet P, Shore KA (1998) Modeling of optical synchronization of chaotic external-cavity VCSEL's. *IEEE J Quantum Electron* 34:1673–1679
- Spencer PS, Mirasso CR (1999) Analysis of optical chaos synchronization in frequency-detuned external-cavity VCSEL's. *IEEE J Quantum Electron* 35:803–809
- Sugawara T, Tachikawa M, Tsukamoto T, Shimizu T (1994) Observation of synchronization in laser chaos. *Phys Rev Lett* 72:3502–3506
- Sukow DW, Gavrielides A, Erneux T, Baracco MJ, Parmenter ZA, Blackburn KL (2005) Two-field description of chaos synchronization in diode lasers with incoherent optical feedback and injection. *Phys Rev A* 72: 043818-1–6
- Sukow DW, Gavrielides A, Erneux T, Mooneyham B, Lee K, McKay J, Davis J (2010) Asymmetric square waves in mutually coupled semiconductor lasers with orthogonal optical injection. *Phys Rev E* 81: 025206-1–4
- Sukow DW, Gavrielides A, McLachlan T, Burner G, Amonette J, Miller J (2006) Identity synchronization in diode lasers with unidirectional feedback and injection of rotated optical fields. *Phys Rev* 74: 023812-1–8
- Sukow DW, Blackburn KL, Spain AR, Babcock KJ, Bennett JV, Gavrielides A (2004) Experimental synchronization of chaos in diode lasers with polarization-rotated feedback and injection. *Opt Lett* 29:2393–2395
- Takiguchi Y, Liu Y, Ohtsubo J (1999a) Low-frequency fluctuations and frequency-locking in semiconductor lasers with optical feedback. *Opt Rev* 6:339–401
- Takiguchi Y, Liu Y, Ohtsubo J (1999b) Low frequency fluctuation in semiconductor lasers with long external cavity feedback and its control. *Opt Rev* 6:424–432
- Takiguchi Y, Fujino H, J. Ohtsubo J, (1999c) Experimental synchronization of chaotic oscillations in external cavity semiconductor lasers in low-frequency fluctuation regime. *Opt Lett* 24:1570–1572
- Takiguchi Y, Ohyagi K, Ohtsubo J (2003) Bandwidth-enhanced chaos synchronization in strongly injection-locked semiconductor lasers with optical feedback. *Opt Lett* 28:319–321
- Takeuchi Y, Shogenji R, Ohtsubo J (2010) Chaos synchronization of semiconductor lasers with polarization-rotated optical feedback and polarization-rotated optical injection. *Opt Rev* 17:467–475
- Tang S, Chen HF, Liu JM (2001) Stable route-tracking synchronization between two chaotically pulsing semiconductor lasers. *Opt Lett* 26:1489–1491

- Tang S, Vicente R, Chiang MC, Mirasso CR, Liu JM (2004) Nonlinear dynamics of semiconductor lasers with mutual optoelectronic coupling. *IEEE J Select Topics Quantum Electron* 10:936–943
- Uchida A, Rogister F, García-Ojalvo J, Roy R (2005) Synchronization and communication with chaotic laser systems. In: Wolf E (ed) *Progress in optics*. Chap. 5, Vol. 48, North-Holland, Amsterdam
- Vicente R, Fischer I, Mirasso CR (2008) Synchronization properties of three delay-coupled semiconductor lasers. *Phys Rev E* 78: 066202-1–11
- Voss HU (2000) Anticipating chaotic synchronization. *Phys Rev E* 61:5115–5119
- Winful HG, Rahman L (1990) Synchronized chaos and spatiotemporal chaos in arrays of coupled lasers. *Phys Rev Lett* 65:1575–1578
- Yamamoto T, Oowada I, Yip H, Uchida A, Yoshimori S, Yoshimura K, Muramatsu J, Goto S, Davis P (2007) Common-chaotic-signal induced synchronization in semiconductor lasers. *Opt Express* 15:3974–3980
- Zhang WL, Pan W, Luo B, Zou XH, Wang MY (2008) One-to-many and many-to-one optical chaos communications using semiconductor lasers. *IEEE Photon Technol Lett* 20:712–714